



# Evidence for distinct proportions of subducted oceanic crust and lithosphere in HIMU-type mantle beneath El Hierro and La Palma, Canary Islands

James M.D. Day<sup>a,b,\*</sup>, D. Graham Pearson<sup>b</sup>, Colin G. Macpherson<sup>b</sup>, David Lowry<sup>c</sup>,  
Juan Carlos Carracedo<sup>d</sup>

<sup>a</sup> Department of Geology, University of Maryland, College Park, MD 20742, USA

<sup>b</sup> Department of Earth Sciences, University of Durham, Durham, DH1 3LE, UK

<sup>c</sup> Department of Earth Sciences, Royal Holloway, University of London, Surrey, TW20 0EX, UK

<sup>d</sup> Estación Volcanologica De Canarias, CSIC, 38206, La Laguna, Tenerife, Spain

Received 9 February 2010; accepted in revised form 13 August 2010

## Abstract

Shield-stage high-MgO alkalic lavas from La Palma and El Hierro (Canary Islands) have been characterized for their O–Sr–Nd–Os–Pb isotope compositions and major-, trace-, and highly siderophile-element (HSE: Os, Ir, Ru, Pt, Pd, Re) abundances. New data are also reported for associated evolved rocks, and entrained xenoliths. Clear differences in Pd/Ir and isotopic ratios for high Os (>50 ppt) lavas from El Hierro ( $\delta^{18}\text{O}_{\text{olivine}} = 5.17 \pm 0.08\text{‰}$ ;  $^{87}\text{Sr}/^{86}\text{Sr} = 0.7029$  to  $0.7031$ ;  $\epsilon_{\text{Nd}} = +5.7$  to  $+7.1$ ;  $^{187}\text{Os}/^{188}\text{Os} = 0.1481$  to  $0.1750$ ;  $^{206}\text{Pb}/^{204}\text{Pb} = 19.1$  to  $19.7$ ; Pd/Ir =  $6 \pm 3$ ) versus those from La Palma ( $\delta^{18}\text{O}_{\text{olivine}} = 4.87 \pm 0.18\text{‰}$ ;  $^{87}\text{Sr}/^{86}\text{Sr} = 0.7031$  to  $0.7032$ ;  $\epsilon_{\text{Nd}} = +5.0$  to  $+6.4$ ;  $^{187}\text{Os}/^{188}\text{Os} = 0.1421$  to  $0.1460$ ;  $^{206}\text{Pb}/^{204}\text{Pb} = 19.5$  to  $20.2$ ; Pd/Ir =  $11 \pm 4$ ) are revealed from the dataset.

Crustal or lithospheric assimilation during magma transport cannot explain variations in isotopic ratios or element abundances of the lavas. Shallow-level crystal–liquid fractionation of olivine, clinopyroxene and associated early-crystallizing minerals (e.g., spinel and HSE-rich phases) controlled compatible element and HSE abundances; there is also evidence for sub-aerial degassing of rhenium. High-MgO lavas are enriched in light rare earth elements, Nb, Ta, U, Th, and depleted in K and Pb, relative to primitive mantle abundance estimates, typical of HIMU-type oceanic island basalts. Trace element abundances and ratios are consistent with low degrees (2–6%) of partial melting of an enriched mantle source, commencing in the garnet stability field ( $\geq 110$  km). Western Canary Island lavas were sulphur undersaturated with estimated parental melt HSE abundances (in ppb) of  $0.07 \pm 0.05$  Os,  $0.17 \pm 0.16$  Ir,  $0.34 \pm 0.32$  Ru,  $2.6 \pm 2.5$  Pt,  $1.4 \pm 1.2$  Pd,  $0.39 \pm 0.30$  Re. These estimates indicate that Canary Island alkali basalts have lower Os, Ir and Ru, but similar Pt, Pd and Re contents to Hawaiian tholeiites.

The HIMU affinities of the lavas, in conjunction with the low  $\delta^{18}\text{O}_{\text{olivine}}$  and high  $^{206}\text{Pb}/^{204}\text{Pb}$  for La Palma, and elevated  $^{187}\text{Os}/^{188}\text{Os}$  for El Hierro implies melting of different proportions of recycled oceanic crust and lithosphere. Our preferred model to explain isotopic differences between the islands is generation from peridotitic mantle metasomatised by <10% pyroxenite/eclogite made from variable portions of similar aged recycled oceanic crust and lithosphere. The correspondence of radiogenic  $^{206}\text{Pb}/^{204}\text{Pb}$ ,  $^{187}\text{Os}/^{188}\text{Os}$ , elevated Re/Os and Pt/Os, and low- $\delta^{18}\text{O}$  in western Canary Island lavas provides powerful support for recycled oceanic crust and lithosphere to generate the spectrum of HIMU-type ocean island basalt signatures. Persistence of geochemical heterogeneities throughout the stratigraphies of El Hierro and La Palma demonstrate long-term preservation of these recycled components in their mantle sources over relatively short-length scales ( $\sim 50$  km).

© 2010 Elsevier Ltd. All rights reserved.

\* Corresponding author at: Department of Geology, University of Maryland, College Park, MD 20742, USA. Tel.: +1 301 405 2707.  
E-mail address: jamesday@geol.umd.edu (J.M.D. Day).

## 1. INTRODUCTION

Mantle heterogeneity undisputedly exists in Earth, but its causes, effects and scales of preservation are poorly resolved. Geochemical studies of ocean island basalts (OIB) offer primary means for understanding mantle heterogeneity (e.g., Gast et al., 1964; Hofmann, 2003), with OIB Sr–Nd–Pb isotope systematics defining mantle components with long-term (>1 Ga) incompatible element enrichment relative to depleted mid-ocean ridge basalt source mantle (depleted MORB mantle or DMM; White, 1985; Zindler and Hart, 1986). These isotopic ‘flavours’ are probably not tightly defined end-members, but instead span a range of isotopic compositions (e.g., Zindler and Hart, 1986; Hofmann, 1997, 2003), reflecting reservoirs distinctive in both age and composition. Such reservoirs are classically interpreted to include recycled oceanic and continental crust and lithosphere, asthenosphere-hosted reservoirs, primitive or modified mantle, and possibly outer core contributions (e.g., Hofmann and White, 1982; Hart, 1984; White, 1985; Hart et al., 1992; Halliday et al., 1995; Brandon and Walker, 2005). It has also been recognized that direct melting of recycled crust and lithosphere cannot readily explain OIB compositions (Niu and O’Hara, 2003). Instead, mixtures of eclogite or pyroxenite with peridotite, or amphibole veins in the oceanic lithosphere, formed by mantle metamorphism, metasomatism and melting have been proposed as OIB mantle source candidates (Halliday et al., 1995; Hauri, 1996; Sobolev et al., 2005, 2007; Spandler et al., 2008; Pilet et al., 2008; Gurenko et al., 2009; Day et al., 2009). OIB are also susceptible to geochemical modification during shallow-level melt transport, when they may be generated from, or interact with, oceanic lithosphere (e.g., O’Hara, 1996; Class and Goldstein, 1997; Widom et al., 1999; Gurenko et al., 2001; Lundstrom et al., 2003), or can assimilate volcanic edifice materials (e.g., Marcantonio et al., 1995; Garcia et al., 1998, 2008; Gaffney et al., 2005; Wang and Eiler, 2008).

The western Canary Islands of El Hierro and La Palma are excellent locations for constraining shallow-level magmatic processes and for understanding OIB mantle source evolution. These islands are in the ‘shield building’ phase of construction, have suffered limited subsidence and are dissected by large structural collapse events, exposing much of their stratigraphy (Carracedo et al., 2001). Both islands have trace element and Sr–Nd isotope systematics consistent with HIMU-type OIB localities (high- $\mu$  = elevated  $^{238}\text{U}/^{204}\text{Pb}$ ), but their lead isotope signatures ( $^{206}\text{Pb}/^{204}\text{Pb}$  = 18.8 to 20.2; Sun, 1980; Hoernle and Tilton, 1991; Marcantonio et al., 1995; Thirlwall et al., 1997; Gurenko et al., 2006) are less radiogenic than ‘classic’ HIMU OIB (St. Helena, Tubuaii and Mangaia;  $^{206}\text{Pb}/^{204}\text{Pb}$  = 20.5 to 22; Graham et al., 1992; Woodhead, 1996). The HIMU-type Pb and radiogenic  $^{187}\text{Os}/^{188}\text{Os}$  isotope signatures in La Palma lavas are considered to reflect melting of ancient to relatively young ( $\leq 2$  Ga) recycled oceanic components in their mantle source (Marcantonio et al., 1995; Widom et al., 1999).

We present new major-, trace-, and highly siderophile-element (HSE: Os, Ir, Ru, Pt, Pd, Re) abundance data,

and O–Sr–Nd–Os–Pb isotopic data for high-MgO ‘shield stage’ alkali basalts, basanites and picrites from La Palma and El Hierro. New data is also presented for mafic-ultramafic xenoliths and evolved lavas and volcanic spines. The advantage of a multi-isotopic and geochemical study of OIB lavas is that it is possible to track different mantle contributions by utilizing the strengths of the varied elemental and isotopic tracers. Oxygen isotope variations in silicate materials are principally sensitive to hydrospheric processes at Earth’s surface, whereas radiogenic Sr–Nd–Os–Pb isotope tracers track long-term parent–daughter fractionation (Rb/Sr, Sm/Nd, Re/Os, U + Th/Pb), with Sr, Nd and Pb isotopes tracking lithophile behaviour and Os isotopes and the HSE being controlled by siderophile and/or chalcophile tendencies. Emphasis is placed on HSE abundances and O–Sr–Nd–Pb–Os isotope systematics, with El Hierro lavas originating from a mantle reservoir with high  $^{187}\text{Os}/^{188}\text{Os}$  ratios (up to 0.175 in basalts with >50 ppt Os), representing a new extreme in OIB multi-isotope space.

## 2. BACKGROUND AND SAMPLES

La Palma and El Hierro are the westernmost Canary Islands (Fig. 1). The Canary Islands show age-progressive volcanism to the west, which has been interpreted as symptomatic of a slow-moving mantle ‘hotspot’ with a low buoyancy flux (Abdel-Monem et al., 1972; Morgan, 1981; Malamud and Turcotte, 1999; Carracedo et al., 2001). This interpretation is corroborated by progressively younger uplifted and exposed submarine seamount stages to the west from Fuerteventura to La Gomera to La Palma (Hoernle and Schmincke, 1993) and progressively older seamounts from Lanzarote to Lars Seamount northeast of the Canary Islands (Geldmacher et al., 2005). The Canary Islands, with the exception of La Gomera, have all experienced Holocene volcanism, and historic eruptions have occurred on La Palma, Tenerife and Lanzarote (Carracedo et al., 2002). La Palma and El Hierro are the only islands currently in the shield building phase of growth.

La Palma lies to the west of the 156 Ma M25 palaeomagnetic anomaly on the youngest oceanic lithosphere of the Canary Islands (Fig. 1). La Palma is composed of two volcanic edifices, the northern Taburiente Shield and the southern Cumbre Vieja Ridge, with a Pliocene Seamount exposed by a giant edifice collapse within the Taburiente Shield (Online Annex, Fig. S1). Recent volcanism has largely been confined to the Cumbre Vieja Ridge (Hernández-Pacheco and Valls, 1982). El Hierro is the smallest and youngest island in the Canary Islands and lies to the east of the M25 anomaly. Studied lavas include generally fresh alkaline picrites, ankaramites, olivine-phyric and hornblende-bearing basanites and basalts, and trachytes. Data for phonolitic spines that outcrop on La Palma, and xenoliths from the two islands are also presented. The detailed stratigraphy and petrography of samples is presented in the Online Annex associated with this article (Section S1, Tables S1 and S2, Figs. S1 and S2).

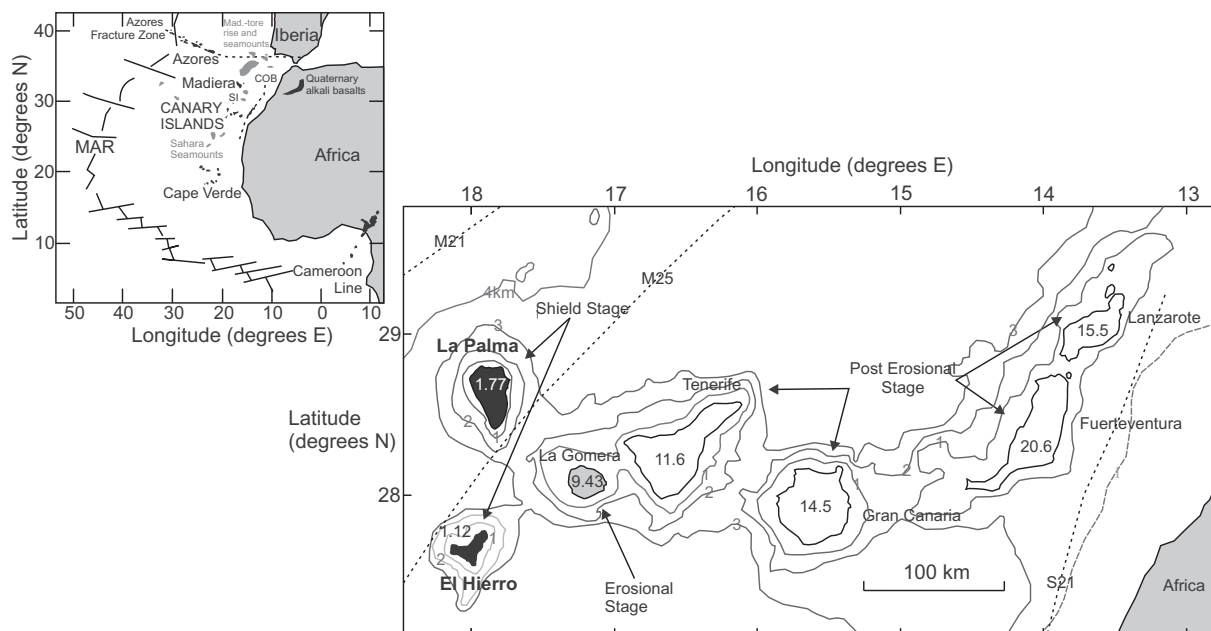


Fig. 1. Map of the Canary Islands and the northwest African continental margin volcanic groups. Current growth stages of the Canary Islands are shown including shield stage (filled), erosional (gray, quiescent) and post-erosional (unfilled; from Carracedo et al., 2002). Numbers within or close to island boundaries represent maximum measured ages for their respective stratigraphies in Ma. Also shown is ocean floor depth (km) and palaeo-magnetic anomalies M25 and S21. S21 lies close to the juncture of the continental/oceanic lithosphere boundary (COB). Inset map shows field of quaternary alkali basalts of the Atlas mountains, possibly related to Canary Island magmatism, the Madiera-Tore rise, Sahara seamounts, Selvagen Islands (SI), Mid-Atlantic Ridge system (MAR), Cameroon line, and the islands of the Canaries, Azores, Madiera and Cape Verde. Maximum measured stratigraphic ages for the Canary Island ages are from Guillou et al. (1996, 1998), Paris et al. (2005) and references therein.

### 3. RESULTS

Detailed analytical methods are presented in the [Online Annex](#) (Section S2, Table S3, Fig. S3). New whole-rock major- and trace-element data are presented in [Table S4](#).

#### 3.1. Major elements

Compositionally, El Hierro lavas range from alkaline basanites and picro-basalts to trachy-andesites, and lavas and volcanic spines from La Palma range from alkaline to highly-alkaline basanites, picro-basalts and picrites to phonolites (Fig. S4). Magnesium contents range from ~0.8 to 28.7 wt.% and *Mg*-number ranges from 26 to 80. Major elements show strong correlation with MgO, consistent with trends for olivine ± clinopyroxene fractional crystallization (Fig. 2). Calculated olivine and clinopyroxene addition for high-MgO lavas are consistent with modal abundances of olivine and clinopyroxene in porphyritic high-MgO lavas (Tables S1 and S2). The strategy for this study was to sample ‘primitive’ mafic and phenocryst-rich lavas, hence the bias toward high-MgO (>8 wt.%) lavas (Fig. S4). The definition of ‘primitive’ used here is those lavas with *Mg*-number >58, >10 wt.% MgO, ≥200 ppm Ni and ≤300 ppm Cr (Lundstrom et al., 2003), which encompasses the majority of the lavas measured for O–Sr–Nd–Os–Pb isotope compositions (11 El Hierro and 15 La Palma lavas). Negative loss on ignition (LOI) measured for El

Hierro and La Palma lavas corroborate petrographic evidence that samples are fresh, suffering limited post-emplacement alteration. The exception is LP03, a visibly altered pillow lava (Fig. S2b), with LOI >6 wt.% from the La Palma Seamount.

Notable differences in major element compositions exist, with El Hierro lavas having elevated TiO<sub>2</sub>, Fe<sub>2</sub>O<sub>3</sub> and P<sub>2</sub>O<sub>5</sub> for a given MgO content than La Palma lavas. This reflects the higher modal abundance of Ti-rich clinopyroxene and magnetite in El Hierro lavas. In a recent compilation of OIB TiO<sub>2</sub> data, Prytulak and Elliott (2007) showed that La Palma lavas have the highest estimated melt Ti concentrations of their compiled OIB dataset (3.0 ± 0.3 wt.% TiO<sub>2</sub>), but made no estimate for El Hierro lavas. La Palma lavas from this study fall in the range of TiO<sub>2</sub> values reported by Prytulak and Elliott (2007). Using data from previously published work, data from this study, and using the method of Prytulak and Elliott (2007), leads us to conclude that El Hierro melts have elevated Ti contents (3.9 ± 0.3 wt.% TiO<sub>2</sub>). Pyroxene- and amphibole-rich xenoliths from La Palma are similar to those described previously (Klügel, 1998) and have increasing TiO<sub>2</sub>, P<sub>2</sub>O<sub>5</sub>, Al<sub>2</sub>O<sub>3</sub> and Fe<sub>2</sub>O<sub>3</sub> abundances with decreasing SiO<sub>2</sub>.

#### 3.2. Trace elements

Compatible trace element (e.g., Ni, Cr, Sc) variations in lavas with greater than ~6 wt.% MgO are controlled by

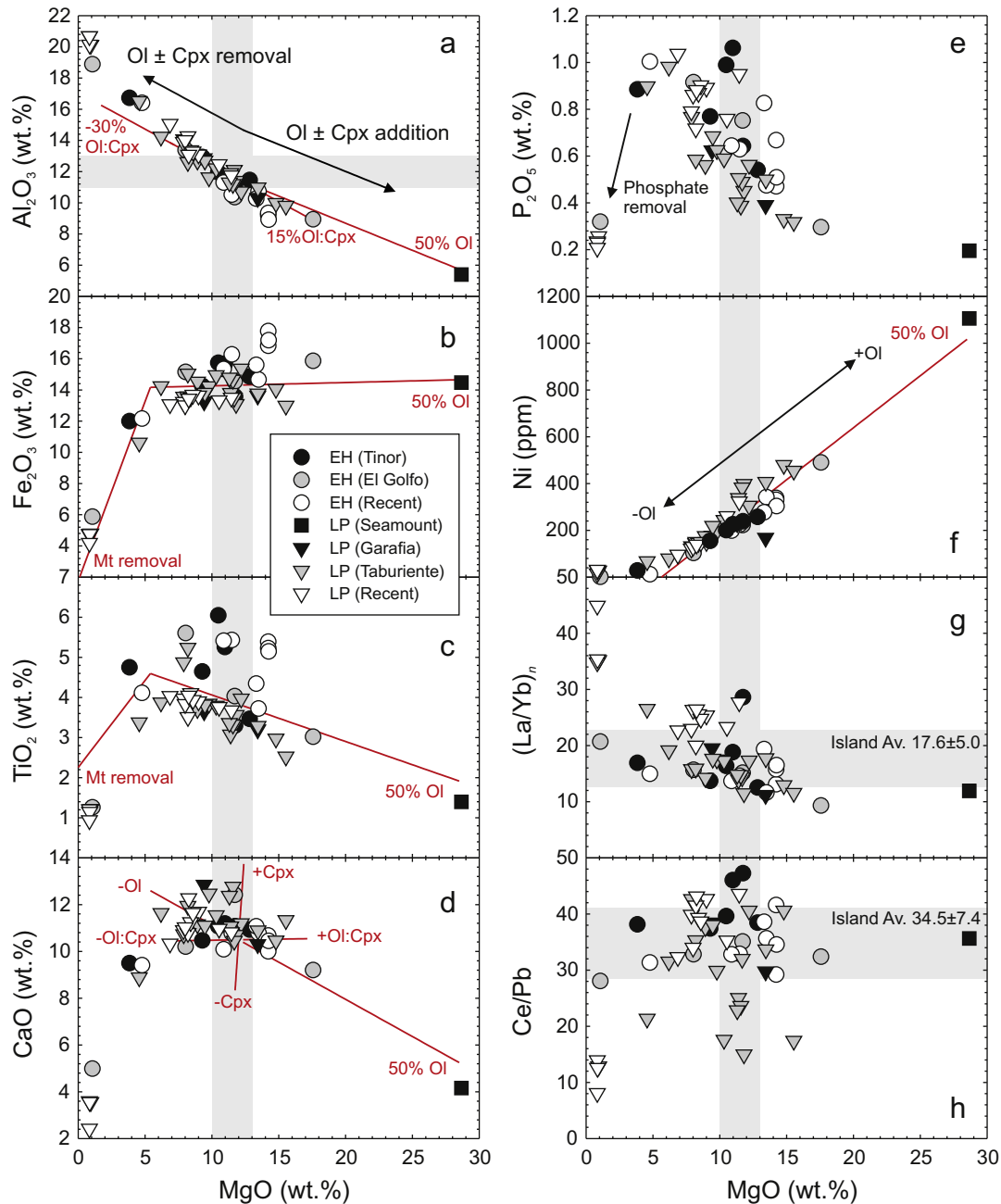


Fig. 2. MgO versus (a)  $\text{Al}_2\text{O}_3$ , (b)  $\text{Fe}_2\text{O}_3$ , (c)  $\text{TiO}_2$ , (d) CaO, (e)  $\text{P}_2\text{O}_5$ , (f) Ni, (g) La/Yb (normalized to primitive mantle; [McDonough and Sun, 1995](#)) and (h) Ce/Pb for La Palma and El Hierro lavas. Calculated removal/addition curves (with maximum percentages conforming to the end of the curves) for olivine (Ol), clinopyroxene (Cpx), and magnetite (Mt) were calculated using measured mineral compositions ([Gurenko et al., 2006](#)). Gray lines indicate estimated parental melt compositions deduced from MgO– $\text{Al}_2\text{O}_3$  relations ([Supplementary material](#)).

fractionation or accumulation of olivine, clinopyroxene and chromite/magnetite (Fig. 2). Ti–augite, magnetite, amphibole and apatite are the primary controlling phases in lavas with  $<6$  wt.% MgO ([Klügel et al., 2000](#)).

El Hierro and La Palma lavas are characterized by similar relative and absolute abundances of trace elements and show similarity to high-MgO lavas from other HIMU ocean island localities, and the Azores (Fig. 3). These char-

acteristics include elevated U, Th, Nb and Ta abundances, and depletions in Pb and K when normalized to primitive mantle (Fig. 3), and represent primary magmatic signatures. Primitive El Hierro ( $(\text{La}/\text{Sm})_n = 2.1$  to 4.7,  $(\text{Nb}/\text{La})_n = 1.2$  to 2.0) and La Palma lavas ( $(\text{La}/\text{Sm})_n = 2.3$  to 4.4,  $(\text{Nb}/\text{La})_n = 1.0$  to 1.6) have steep rare earth element (REE) profiles that are consistent with melting in the presence of garnet. There is limited variation in the absolute

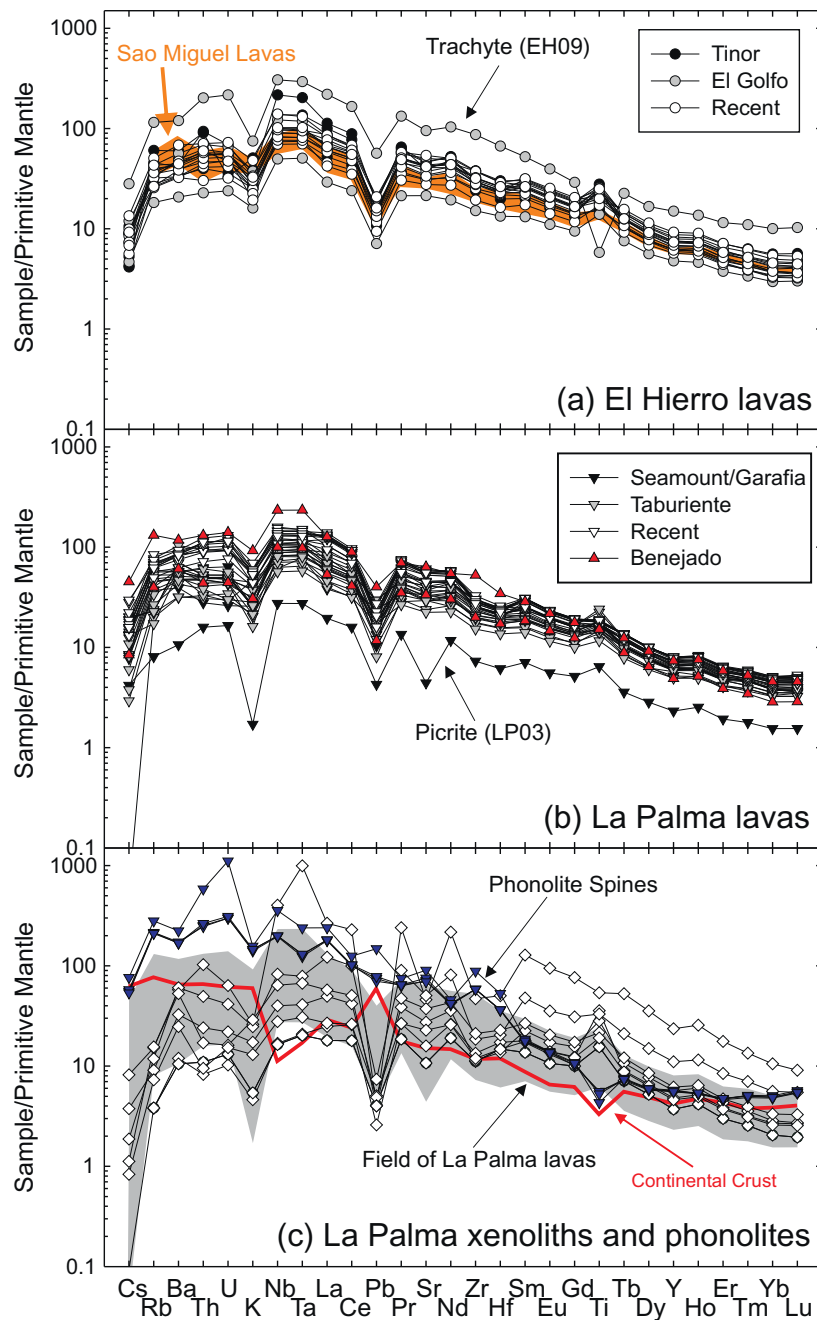


Fig. 3. Primitive mantle normalized multi-element variation diagrams for (a) El Hierro lavas, (b) La Palma lavas and (c) La Palma phonolites and mafic xenoliths. Range of compositions of lavas from Sao Miguel, Azores (panel a: Elliott et al., 2007), and the average continental crust estimate (panel c: Rudnick and Gao, 2003) shown for comparison. Data are normalized to primitive mantle values from McDonough and Sun (1995).

and relative abundances of trace elements both temporally and spatially for the two islands, with two exceptions. First, recent lavas erupted on the Cumbre Vieja ridge of La Palma have higher absolute trace element abundances, and less pronounced U, Th, Ba and Rb depletion relative to Nb and Ta, compared with lavas erupted on the northern Taburiente shield volcano (recent lavas, Fig. 3b). It is notable that Cumbre Vieja lavas, as well as some Benejado lavas, contain amphibole, which broadly correlates with trace ele-

ment abundances. Second, relatively fresh ~700 Ka Iscagua and Fagundo lavas (Taburiente shield) have the lowest Ce/Pb ratios, possibly reflecting elevated Pb or low Ce abundances (Fig. 2h).

Primitive La Palma ( $Nb/U = 59 \pm 14$ ;  $Ce/Pb = 33 \pm 8$ ;  $Nd/Pb = 17 \pm 4$ ;  $Zr/Nb = 3.9 \pm 0.5$ ; 1 St. Dev.) and El Hierro lavas ( $Nb/U = 70 \pm 22$ ;  $Ce/Pb = 37 \pm 5$ ;  $Nd/Pb = 21 \pm 2$ ;  $Zr/Nb = 4.7 \pm 0.8$ ) have trace element ratios that overlap and extend to more extreme values than

Table 1  
Sr–Nd–Pb isotope data for El Hierro and La Palma lavas.

Sample	Series	Age (Ka)	MgO	$^{87}\text{Sr}/^{86}\text{Sr}$	( $\pm 1\sigma$ )	$^{143}\text{Nd}/^{144}\text{Nd}$	( $\pm 1\sigma$ )	$^{206}\text{Pb}/^{204}\text{Pb}$	( $\pm 1\sigma$ )	$^{207}\text{Pb}/^{204}\text{Pb}$	( $\pm 1\sigma$ )	$^{208}\text{Pb}/^{204}\text{Pb}$	( $\pm 1\sigma$ )
<i>El Hierro, western Canary Islands, Spain</i>													
JMDD EH01	PFE	<1	14.2	0.702976	0.000004	0.512982	0.000006	19.358	0.002	15.596	0.002	39.014	0.005
JMDD EH03	Tinõr	1030	12.8	0.702960	0.000006	0.512966	0.000003	19.392	0.004	15.571	0.003	39.023	0.008
JMDD EH07	Tinõr	1030	11.7	0.703042	0.000004	0.512993	0.000004	19.134	0.002	15.567	0.002	38.878	0.005
JMDD EH10	CFE	160	14.2	0.702990	0.000005	0.512942	0.000003	19.597	0.007	15.584	0.006	39.244	0.014
JMDD EH11	CFE	160	11.5	0.703020	0.000004	0.512930	0.000003	19.634	0.001	15.610	0.001	39.334	0.002
JMDD EH12	CFE	135	13.5	0.703040	0.000005	0.512959	0.000004	19.291	0.008	15.531	0.006	38.933	0.017
JMDD EH13	CFE	135	14.2	0.703013	0.000005	0.512940	0.000002	19.532	0.002	15.596	0.002	39.209	0.004
JMDD EH14	UEG	265	8.03	0.702984	0.000005	0.512968	0.000003	19.332	0.005	15.562	0.004	39.018	0.009
JMDD EH15	UEG	335	17.6	0.703044	0.000005	0.512973	0.000004	19.462	0.002	15.593	0.002	39.167	0.005
JMDD EH16	LEG	540	11.7	0.702871	0.000005	0.513003	0.000003	19.109	0.002	15.561	0.002	38.727	0.005
JMDD EH17	PFE	<10	13.3	0.702989	0.000004	0.512956	0.000003	19.409	0.009	15.570	0.007	39.089	0.018
JMDD EH18	PFE	<1	10.9	0.703144	0.000005	0.512952	0.000005	19.666	0.001	15.617	0.001	39.348	0.003
<i>La Palma, western Canary Islands, Spain</i>													
JMDD LP01	Garafia	1440	13.4	0.703057	0.000004	0.512914	0.000004	19.759	0.001	15.627	0.001	39.704	0.002
JMDD LP02	Garafia	1440	9.43	0.703150	0.000005	0.512930	0.000004	20.152	0.001	15.659	0.001	39.882	0.002
JMDD LP03 (ul)	Seamount	3000	28.7	0.703964	0.000004	0.512966	0.000017	19.698	0.007	15.596	0.006	39.292	0.014
Replicate (l)				0.703218	0.000004								
JMDD LP04	L. Tab.	1020	7.90	0.703091	0.000004	0.512897	0.000003	19.909	0.001	15.627	0.001	39.695	0.003
JMDD LP05	L. Tab.	1020	12.2	0.703062	0.000005	0.512920	0.000003	19.720	0.001	15.619	0.001	39.468	0.003
JMDD LP07	L. Tab.	1020	9.79	0.703062	0.000006	0.512896	0.000003	19.842	0.001	15.626	0.001	39.721	0.002
JMDD LP09	Benejado	490	13.5	0.703221	0.000004	0.512905	0.000003	20.141	0.001	15.657	0.001	40.014	0.003
JMDD LP14	CFE	120	11.5	0.703117	0.000004	0.512923	0.000002	19.527	0.003	15.592	0.002	39.277	0.006

(ul) = Unleached powder of LP03; (l) = leached powder of LP03 (see Analytical methods, Section S2 for details).

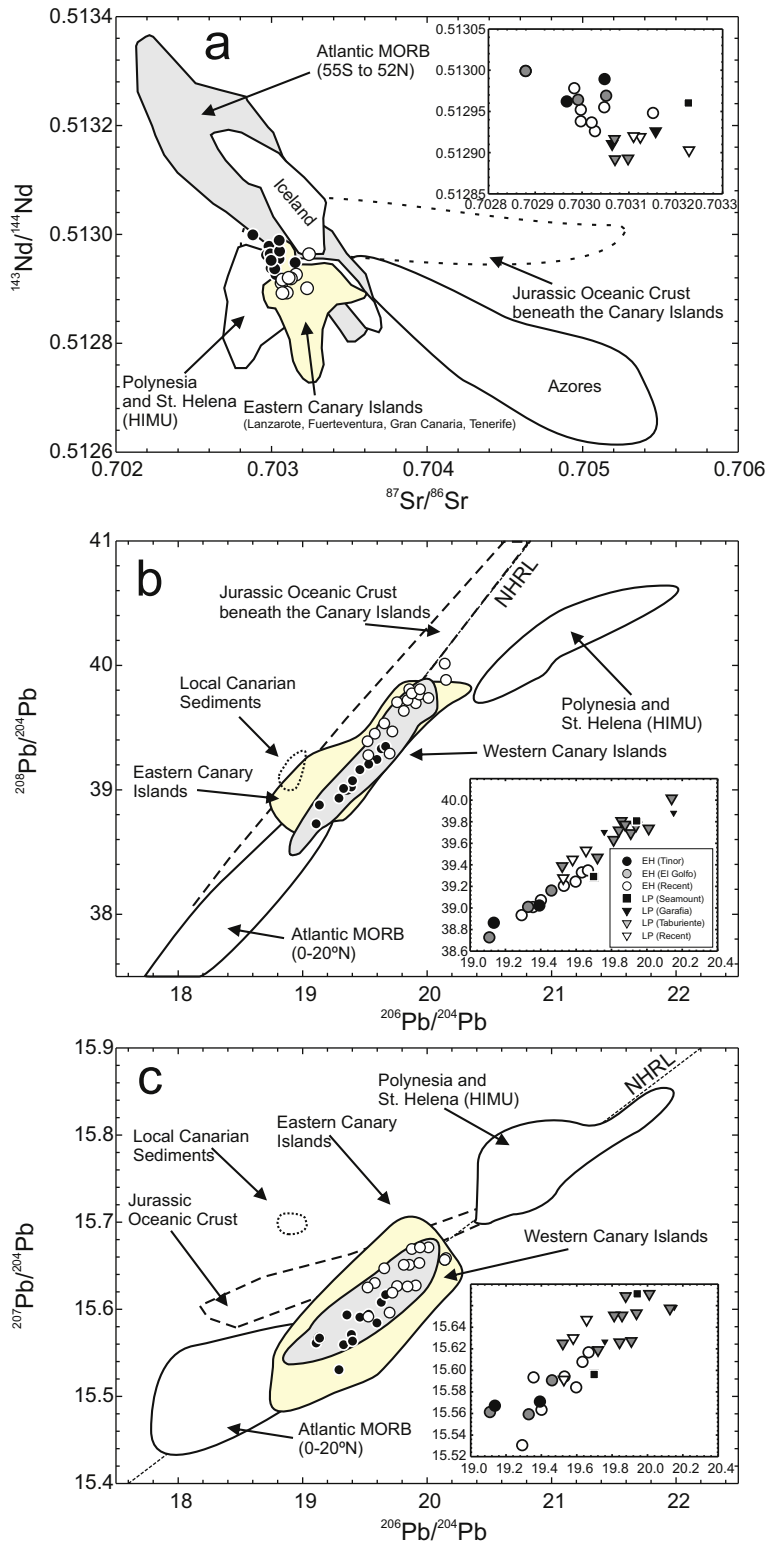


Fig. 4. (a)  $^{87}\text{Sr}/^{86}\text{Sr}$  versus  $^{143}\text{Nd}/^{144}\text{Nd}$ , and  $^{206}\text{Pb}/^{204}\text{Pb}$  versus (b)  $^{208}\text{Pb}/^{204}\text{Pb}$  and (c)  $^{207}\text{Pb}/^{204}\text{Pb}$  diagrams for La Palma (unfilled circles) and El Hierro lavas (filled circles; inset panels show samples by stratigraphic unit). Comparison data from: Northern hemisphere reference line (NHRL; Hart, 1984), published La Palma and El Hierro data (Sun, 1980; Whitehouse and Neumann, 1995; Marcantonio et al., 1995), MORB (PET-DB database; <http://www.petdb.org>), eastern Canary Island and local sediment data (Thirlwall et al., 1997, and references therein); Data for HIMU from Hauri and Hart (1993), Azores and Iceland from Elliott et al. (2007), and references therein.  $2\sigma$  errors are smaller than symbols.

average global OIB and MORB ( $\text{Nb}/\text{U} = 47 \pm 10$ ;  $\text{Ce}/\text{Pb} = 25 \pm 5$ ;  $\text{Nd}/\text{Pb} = 24 \pm 5$ ; Hofmann et al., 1986; Rehkämper and Hofmann, 1997; Hofmann, 2003), but that are similar to extreme HIMU OIB and to some Azorean lavas (Elliott et al., 2007). Trace element ratios for El Hierro and La Palma lavas differ from some Gran Canaria lavas that are considered to have a strong continental sediment signature (Thirlwall et al., 1997;  $\text{Nb}/\text{U} = 52 \pm 8$ ;  $\text{Ce}/\text{Pb} = 42 \pm 7$ ;  $\text{Zr}/\text{Nb} = 7.7 \pm 0.7$ ), or that may reflect the

presence of recycled oceanic crust in their mantle source (Hoernle, 1998).

On La Palma, evolved hauyne-bearing phonolites display distinctive geochemistry to mafic rocks. The phonolites lack negative Pb anomalies, have minor negative K, Ti and Ta anomalies, positive U, Th, Sr and Zr anomalies, elevated large ion lithophile element (LILE) and HFSE abundances, and relatively flat, concave-up REE patterns that are similar to those estimated for bulk continental crust;

Table 2  
Oxygen isotope results for El Hierro and La Palma lavas and xenoliths.

Sample	Series	$\delta^{18}\text{O}_{\text{OI}}$	( $\pm 2\sigma$ )	$\delta^{18}\text{O}_{\text{Cpx}}$	( $\pm 2\sigma$ )	$\delta^{18}\text{O}_{\text{Mt}}$	$\Delta^{18}\text{O}_{\text{OI-Cpx}}$	$\Delta^{18}\text{O}_{\text{OI-Mt}}$
<i>El Hierro, western Canary Islands, Spain</i>								
JMDD EH01	PFE	5.26	–	5.59	–	–	–0.33	–
JMDD EH03	Tinör	5.12	–	–	–	–	–	–
JMDD EH04cii	Tinör Xenolith	5.18	0.04	–	–	3.35 <sup>a</sup>	–	1.83 <sup>b</sup>
JMDD EH07	Tinör	5.32	0.03	5.48	–	–	–0.16	–
JMDD EH08	Tinör	5.21	–	5.39	–	–	–0.18	–
JMDD EH10	CFE	5.04	–	5.41	–	–	–0.37	–
JMDD EH11	CFE	5.22	–	5.39	–	–	–0.17	–
JMDD EH12	CFE	5.23	–	–	–	–	–	–
JMDD EH13	CFE	5.15	–	5.37	–	–	–0.22	–
JMDD EH14	UEG	5.13	–	–	–	–	–	–
JMDD EH15	UEG	5.08	0.09	5.44	–	–	–0.36	–
JMDD EH16	LEG	5.08	–	5.27	–	–	–0.19	–
JMDD EH17	PFE	5.13	–	–	–	–	–	–
JMDD EH18	PFE	5.26	–	5.40	–	–	–0.14	–
<i>La Palma, western Canary Islands, Spain</i>								
JMDD LP01	Garafia	4.88	–	5.12	–	–	–0.24	–
JMDD LP02	Garafia	4.73	0.15	5.01	–	–	–0.28	–
JMDD LP03	Seamount	5.00	–	–	–	–	–	–
JMDD LP04	L. Tab.	4.74	–	5.05	–	–	–0.31	–
JMDD LP05	L. Tab.	4.86	–	5.00	0.12	–	–0.14	–
JMDD LP07	L. Tab.	4.72	–	–	–	–	–	–
JMDD LP09	Benejado	4.93	–	5.02	–	–	–0.09	–
JMDD LP10	U. Tab.	4.90	–	–	–	–	–	–
JMDD LP11	U. Tab.	4.71	–	–	–	–	–	–
JMDD LP13A	CFE Xenolith	4.36	–	4.92	–	–	–0.56	–
JMDD LP13B	CFE Xenolith	4.80	–	5.04	–	–	–0.24	–
JMDD LP14	CFE	4.90	–	–	–	–	–	–
JMDD LP15	1949 San Juan Flow	4.92	–	–	–	–	–	–
JMDD LP19	Birigoyo	4.79	–	–	–	–	–	–
JMDD LP21bi	San Antonio Xeno.	4.58	–	5.27	–	–	–0.69	–
JMDD LP23	1971 Flow	4.92	–	–	–	–	–	–
JMDD LP24	1677 Flow	4.96	–	–	–	–	–	–
JMDD LP25	1646 Flow	5.02	–	–	–	–	–	–
LP96-66	U. Tab.	4.83	–	5.14	–	–	–0.31	–
LP96-46	Tab.	4.90	0.06	5.42	0.03	–	–0.52	–
LP 69E	1949 San Juan Flow	5.01	0.10	5.17	0.11	3.70	–0.16	1.31
LP 30B	1712 Flow	–	–	–	–	3.16	–	–
LP 95B	1585 Flow	–	–	–	–	3.41	–	–
LP 41D	1971 Flow	–	–	–	–	3.44	–	–
LP 105	Tab.	4.93	0.13	–	–	–	–	–
LP 106	Tab.	4.99	0.15	5.75	0.21	–	–0.76	–
LP 107	Tab.	5.35	–	5.49	0.07	–	–0.14	–
LP 110	Tab.	5.01	0.08	5.23	–	–	–0.22	–
LP 113	Tab.	4.76	0.01	5.16	0.01	–	–0.40	–
LP 116	Tab.	–	–	–	–	3.46	–	–
LP 134	Seamount	4.89	0.06	5.39	0.06	–	–0.50	–

<sup>a</sup> Chromite analysis.

<sup>b</sup>  $\delta^{18}\text{O} = \text{OI-Cr}$ .



LILE and HFSE abundances and ratios differ significantly from bulk continental crust, however (Fig. 3). La Palma xenoliths span a range of absolute and relative trace element abundances, with more extreme HFSE, Pb and Sr anomalies compared with associated lavas. Pyroxenite and amphibole-bearing xenoliths have generally higher Ce/Pb, La/Nb and lower Th/U than their host lavas (Table S4).

### 3.3. Strontium, neodymium and lead isotopes

All lavas yield  $^{87}\text{Sr}/^{86}\text{Sr}$  and  $^{143}\text{Nd}/^{144}\text{Nd}$  ratios within the range of previously published Canary Island and HIMU-type OIB (Table 1; Fig. 4). For LP03, leaching was required to remove the effect of seawater alteration (Section S2) that did not affect Nd, Pb, Os or O isotope compositions. El Hierro lavas have  $^{87}\text{Sr}/^{86}\text{Sr}$  ranging from 0.70287 to 0.70314 and  $\epsilon_{\text{Nd}} = +5.7$  to  $+7.1$ . La Palma lavas have  $^{87}\text{Sr}/^{86}\text{Sr}$  ranging from 0.70306 to 0.70322 and  $\epsilon_{\text{Nd}} = +5.0$  to  $+6.4$ . Pb isotope data are plotted in Fig. 4. Data for both islands fall along, or below, the northern hemisphere reference line (NHRL; Hart, 1984), with  $\Delta^{7/4} = +0.6$  to  $-5.2$  and  $-0.6$  to  $-3.0$  and  $\Delta^{8/4} = +11.8$  to  $-7.6$  and  $+18.8$  to  $-15.0$  for El Hierro and La Palma lavas, respectively. The new Pb isotope dataset spans almost the entire range measured for Canary Island lavas ( $^{206}\text{Pb}/^{204}\text{Pb} = 18.8$  to  $20.2$ ; Sun, 1980; Hoernle and Tilton, 1991; Hoernle et al., 1991; Marcantonio et al., 1995; Thirlwall et al., 1997; Gurenko et al., 2006). Overall characteristics in Pb-isotope space are that El Hierro lavas have generally less radiogenic  $^{87}\text{Sr}/^{86}\text{Sr}$  and Pb and higher  $^{143}\text{Nd}/^{144}\text{Nd}$  isotope compositions than La Palma lavas. Western Canary Island lavas lie in the upper range of HIMU-type OIB Sr–Nd isotope compositions and possess a more restricted and less radiogenic range of  $^{143}\text{Nd}/^{144}\text{Nd}$  than eastern Canary Island lavas. Additionally, there is no evidence for a component with high- $^{207}\text{Pb}/^{204}\text{Pb}$  in La Palma or El Hierro lavas. This high- $^{207}\text{Pb}/^{204}\text{Pb}$  feature, seen in eastern Canary Island lavas, has been attributed either to enriched lithosphere (Hoernle et al., 1991), or sedimentary materials (Thirlwall et al., 1997).

### 3.4. Oxygen isotopes

Laser fluorination oxygen isotope analyses are presented for fresh, pre-fluorinated mineral separates from La Palma and El Hierro lavas and xenoliths in Table 2. The range of  $\delta^{18}\text{O}$  values in olivine and clinopyroxene phenocrysts from La Palma lavas is more variable and  $\sim 0.3\text{‰}$  lower ( $\delta^{18}\text{O}_{\text{Ol}} +4.87 \pm 0.18\text{‰}$ ;  $n = 27$ ;  $\delta^{18}\text{O}_{\text{Cpx}} +5.20 \pm 0.11\text{‰}$ ;  $n = 16$ , 1 St. Dev.) than for El Hierro lavas ( $\delta^{18}\text{O}_{\text{Ol}} +5.17 \pm 0.08\text{‰}$ ;  $n = 14$ ;  $\delta^{18}\text{O}_{\text{Cpx}} +5.42 \pm 0.09\text{‰}$ ;  $n = 9$ ) (Fig. 5). Magnetite separates from La Palma exhibit a range in  $\delta^{18}\text{O}$  ( $+3.43 \pm 0.19\text{‰}$ ;  $n = 5$ ) and a single chromite analysed from an El Hierro dunite xenolith gave a  $\delta^{18}\text{O}$  value of  $+3.35\text{‰}$ . The range of  $\Delta^{18}\text{O}_{\text{Ol-Cpx}}$  values are similar for the two islands (La Palma lavas =  $-0.35 \pm 0.20$ ; El Hierro lavas =  $-0.24 \pm 0.09$ ). Only one sample was analysed for olivine, clinopyroxene and magnetite, and gave

$\Delta^{18}\text{O}_{\text{Ol-Mt}} = 1.31$  and  $\Delta^{18}\text{O}_{\text{Ol-Cpx}} = -0.16$ . These values lie within the extrapolated field for isotopic equilibrium deduced from olivine-clinopyroxene pairs in peridotite nodules (Mattey et al., 1994; Fig. S5). Single  $\Delta^{18}\text{O}_{\text{Ol-Cr}}$  (1.83) and  $\Delta^{18}\text{O}_{\text{Ol-Mt}}$  (1.31) coupled measurements are similar to

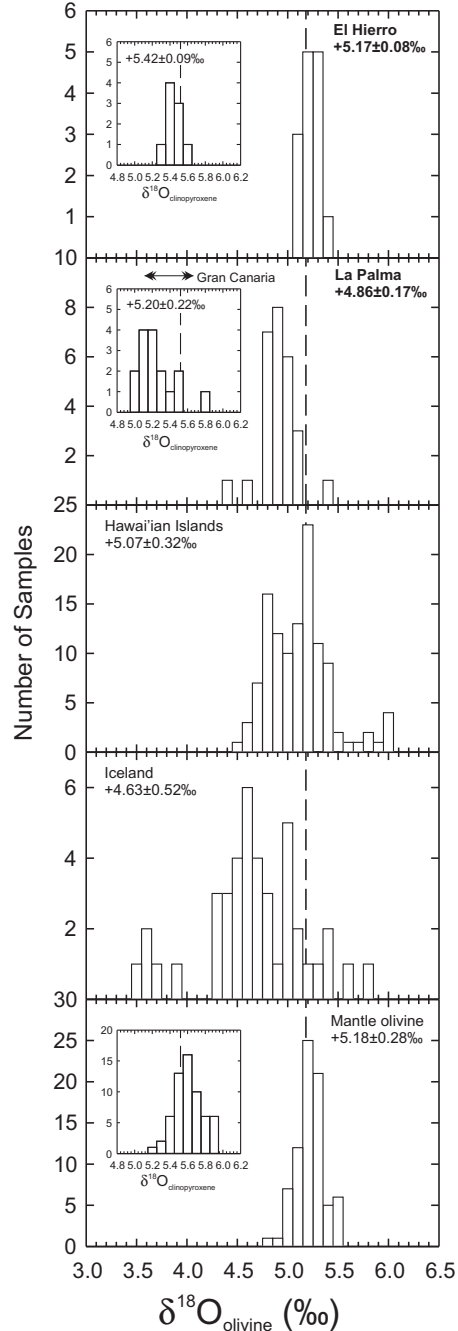


Fig. 5. Histograms of  $\delta^{18}\text{O}_{\text{olivine}}$  for El Hierro, La Palma, Hawaiian Islands, Iceland and olivine from mantle nodules. Insets show histograms of  $\delta^{18}\text{O}_{\text{clinopyroxene}}$  for the same islands and for mantle nodules along with the range of  $\delta^{18}\text{O}_{\text{clinopyroxene}}$  measured in Gran Canaria lavas (from Thirlwall et al. (1997)). Mantle nodule olivine and pyroxene data from Mattey et al. (1994), Hawaiian and Icelandic data compilations from Eiler et al. (1996), Macpherson et al. (2005), Gaffney et al. (2005), and references therein.

olivine-oxide pairs from mafic-ultramafic intrusions (Lowry et al., 2003; Day et al., 2008a). Oxygen isotope ratios for El Hierro lavas lie within the range of mantle peridotites

(Mattey et al., 1994) and MORB (Eiler et al., 2000), whereas La Palma lavas extend to more  $^{18}\text{O}$ -depleted signatures (Fig. 5).

Table 3

Osmium isotope and highly siderophile-element abundance data for western Canary Island rocks.

Sample	Rock type	Os (ppb)	Ir (ppb)	Ru (ppb)	Pt (ppb)	Pd (ppb)	Re (ppb)	$^{187}\text{Os}/^{188}\text{Os}_m$	$2\sigma$
<i>El Hierro, western Canary Islands, Spain</i>									
JMDD EH 01	Ankaramite	0.065	0.065	0.131	0.430	0.632	0.473	0.14579	0.00015
Repeat		0.073	–	–	–	–	0.486	0.14640	0.00005
JMDD EH 03	Basanite	0.133	–	–	–	–	0.287	0.16760	0.00048
JMDD EH 04	Alkali Basalt	0.060	–	–	–	–	0.447	0.15080	0.00003
JMDD EH 04 c ii	Dunite (X)	0.634	–	–	–	–	0.019	0.13995	0.00008
JMDD EH 07	Ankaramite	0.095	0.090	0.205	1.135	0.064	0.275	0.16686	0.00002
JMDD EH 08	Basanite	0.026	0.166	0.134	0.942	0.407	0.248	0.16286	0.00012
JMDD EH 10	Ankaramite	0.184	–	–	–	–	0.188	0.14808	0.00005
JMDD EH 11	Alkali Basalt	0.055	–	–	–	–	0.337	0.15202	0.00007
JMDD EH 12	Alkali Basalt	0.141	–	–	–	–	0.105	0.17502	0.00006
Repeat		0.088	–	–	–	–	0.138	0.17506	0.00006
JMDD EH 13	Ankaramite	0.058	0.069	1.242	0.556	0.273	0.251	0.16438	0.00006
JMDD EH 14	Alkali Basalt	0.024	0.084	0.093	4.580	0.712	0.462	0.15397	0.00001
JMDD EH 15	Ankaramite	0.158	–	–	–	–	0.121	0.15895	0.00004
Repeat		0.176	–	–	–	–	0.089	0.15648	0.00019
JMDD EH 16	Basanite	0.089	0.168	0.187	1.922	1.459	0.226	0.15693	0.00005
Repeat		0.097	–	–	–	–	0.185	0.15619	0.00002
JMDD EH 17	Alkali Basalt	0.041	–	–	–	–	0.155	0.13874	0.00051
Repeat		0.039	0.040	0.100	0.608	0.414	0.159	0.13914	0.00025
JMDD EH 18	Ankaramite	0.099	0.064	1.361	4.100	0.430	0.482	0.15297	0.00006
<i>La Palma, western Canary Islands, Spain</i>									
JMDD LP 01	Ankaramite	0.143	0.178	0.619	2.402	1.670	0.188	0.14328	0.00001
Repeat		0.103	0.209	0.639	3.069	1.729	0.185	0.14456	0.00006
JMDD LP 02	Ankaramite	0.060	–	–	–	–	0.478	0.14875	0.00007
JMDD LP 03	Picrite pillow lava	0.285	–	–	–	–	0.271	0.14406	0.00001
JMDD LP 04	Ankaramite	0.032	0.223	0.060	2.517	0.730	0.455	0.14788	0.00017
JMDD LP 05	Ankaramite	0.023	–	–	–	–	0.461	0.13783	0.00057
JMDD LP 07	Ankaramite	0.053	–	–	–	–	0.377	0.14532	0.00002
JMDD LP 09	Amphibole-Tephrite	0.157	–	–	–	–	0.067	0.14582	0.00006
JMDD LP 10	Ankaramite	0.077	0.361	0.208	5.644	2.264	0.044	0.14584	0.00006
JMDD LP 11	Basanite	0.052	0.332	0.113	7.903	2.017	0.253	0.14895	0.00005
JMDD LP 13a	Clinopyroxenite (X)	0.131	–	–	–	–	0.198	0.14723	0.00010
JMDD LP 13b	Clinopyroxenite (X)	0.015	–	–	–	–	0.223	0.14434	0.00016
JMDD LP 14	Basanite	0.066	–	–	–	–	0.473	0.14162	0.00024
JMDD LP 15	Basanite	0.053	–	–	–	–	0.197	0.14356	0.00006
JMDD LP 19	Basanite	0.016	–	–	–	–	0.719	0.14858	0.00010
JMDD LP 19X	Hornblendite (X)	0.051	–	–	–	–	0.395	0.14363	0.00011
JMDD LP 21a	Basanite	0.040	–	–	–	–	0.949	0.15614	0.00007
Repeat		0.040	–	–	–	–	0.270	0.15827	0.00008
JMDD LP 21bi	Hornblendite (X)	0.004	–	–	–	–	1.126	0.14049	0.00023
JMDD LP 24	Basanite	0.054	–	–	–	–	0.602	0.13793	0.00009
LP 96-66	Ankaramite	0.209	0.366	0.384	5.894	5.519	0.231	0.14380	0.00031
Repeat		0.209	0.372	0.359	5.812	4.528	0.216	0.14214	0.00015
LP 96-46	Basanite	0.083	0.128	0.229	0.753	1.334	0.267	0.14423	0.00094
LP 96-41	Basanite	0.308	0.204	1.038	1.597	1.275	0.368	0.14387	0.00009
LP 96-63	Basanite	0.207	0.316	0.660	2.643	3.747	0.488	0.14601	0.00010
LP 96-48	Basanite	0.053	0.103	0.044	1.371	1.165	0.263	0.14834	0.00017
LP 96-14	Basanite	0.070	0.128	0.222	1.370	2.095	0.311	0.15480	0.00017
LP 96-22	Basanite	0.070	0.194	0.240	2.670	2.741	0.410	0.14486	0.00013
LP 96-83	Basanite	0.096	0.234	0.660	2.347	3.939	0.493	0.14172	0.00049
<i>EN026 10D-3 MORB reference material</i>									
EN026 10D-3	MORB Basalt	0.007	–	–	–	–	1.062	0.15096	0.00015
EN026 10D-3	MORB Basalt	0.008	–	–	–	–	1.113	0.14926	0.00013
EN026 10D-3	MORB Basalt	0.009	–	–	–	–	1.177	0.14674	0.00013
EN026 10D-3	MORB Basalt	0.059	–	–	–	–	1.044	0.12773	0.00006

(X) = xenolith.

### 3.5. Highly siderophile-element abundances and Re–Os isotopes

Whole-rock Re–Os isotope and highly siderophile-element (HSE: Os, Ir, Ru, Pt, Pd, Re) abundance measurements for La Palma and El Hierro lavas and xenoliths are presented in Table 3. In order to investigate temporal and spatial variations in the two islands, HSE abundances of Taburiente series lavas in La Palma and the full age spectrum of lavas in El Hierro were measured. Seven samples were analysed in duplicate and close agreement was found for Re (<30% 1 St. Dev. variation with the exception of 1 sample) and Os concentrations (<10% 1 St. Dev. variation with the exception of 2 samples) and Os isotopes (<2‰ 1 St. Dev. variation). Variations in concentration probably reflect the ‘nugget effect’ from the heterogeneous distribution of HSE-rich micro-inclusions within sample powders inherited from the bulk rock.

Standards prepared with samples include the peridotite reference material, GP13, which showed excellent agreement with previously published values (data presented in Day et al., 2008a), and the mid-ocean ridge basalt (MORB) reference material EN02610D-3 from the mid-Atlantic ridge, which was measured for Re and Os abundances

and  $^{187}\text{Os}/^{188}\text{Os}$  (Table 3). This reference material was found to be heterogeneous with respect to HSE abundances and Os isotopic composition, as previous workers have demonstrated (Section S3; Table S4), with the new data from this study yielding an isochron with an apparent age of  $2.2 \pm 0.3$  Ma and initial  $^{187}\text{Os}/^{188}\text{Os} = 0.1246 \pm 4$  (MSWD = 0.44; Fig. S6). The initial composition lies close to abyssal peridotite compositions (e.g., Brandon et al., 2000) and to MORB sulphides (Gannoun et al., 2007). The heterogeneous composition of EN02610D-3 is thus considered to reflect sulphide nuggetting within the reference powder.

Absolute abundances of the HSE for western Canary Island lavas are generally greater than for MORB (Bézou et al., 2005; Gannoun et al., 2007), and approach the concentrations measured for Hawaiian picrites (Bennett et al., 2000; Ireland et al., 2009). Concentrations of the HSE in El Hierro and La Palma samples are generally lower than estimates for the primitive upper mantle (PUM; Becker et al., 2006). El Hierro and La Palma lavas have relative enrichments of Pt, Pd and Re compared to Os, Ir and Ru, resulting in positively sloping HSE profiles (Fig. 6;  $(\text{Pt}/\text{Os})_n = 22 \pm 33; 21 \pm 21$ ,  $(\text{Pd}/\text{Os})_n = 9 \pm 8; 20 \pm 9$  and  $(\text{Re}/\text{Os})_n = 55 \pm 53; 89 \pm 120$  for El Hierro and La Palma,

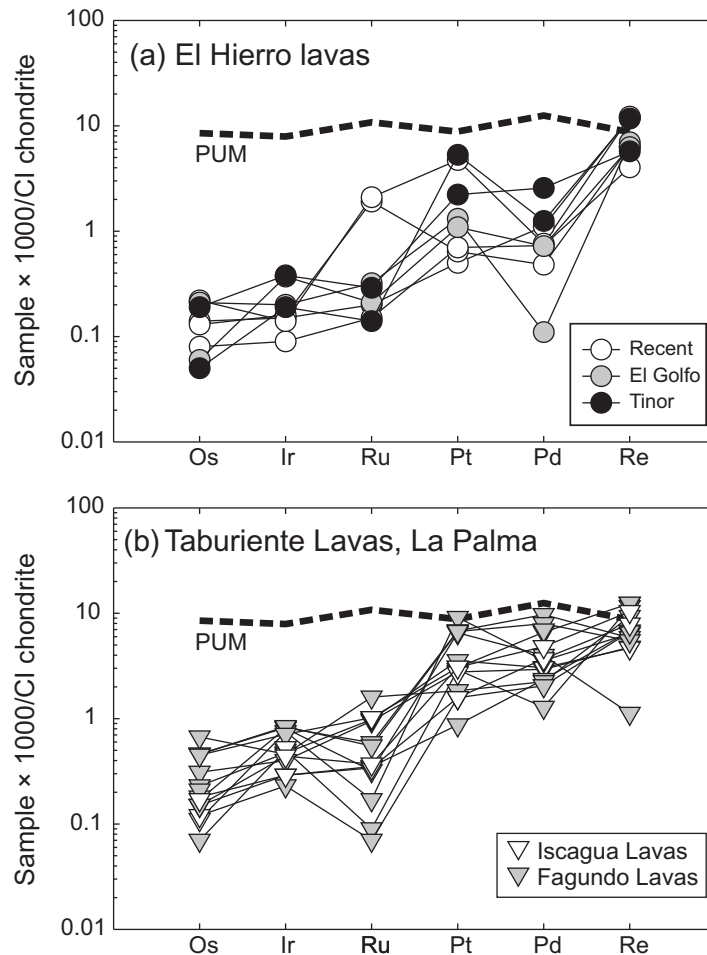


Fig. 6. Highly siderophile element patterns for (a) El Hierro and (b) La Palma Taburiente shield lavas. Data are shown relative to primitive upper mantle (PUM) values from Becker et al. (2006) and normalized relative to CI chondrite, Orgueil (Horan et al., 2003).

respectively;  $n$  = normalized to CI chondrite, Orgueil; Horan et al., 2003). There is only limited evidence for fractionation between Os, Ir and Ru in El Hierro and La Palma lavas ( $(\text{Ir}/\text{Os})_n = 2 \pm 2$  and  $1.7 \pm 0.6$ ;  $(\text{Ru}/\text{Os})_n = 5 \pm 5$  and  $2 \pm 1$ , respectively). The most striking differences between HSE profiles for the two islands is the pronounced depletion of Pd in some El Hierro lavas ( $\text{Pd}/\text{Ir} = 6.4 \pm 3.3$ ; Fig. 6a) relative to La Palma lavas ( $\text{Pd}/\text{Ir} = 10.6 \pm 4.0$ ; Fig. 6b). Pd depletions, relative to Pt and Ir, have also been measured for some Philippine Sea Plate OIB with enriched mantle trace element signatures (Dale et al., 2008), and in high-pressure metamorphic gabbroic eclogites (Dale et al., 2009).

Osmium is positively correlated with MgO (Fig. 7), Ni and modal olivine (Fig. S7), whereas Re generally shows limited correlation with Ni and MgO. Iridium, Ru, Pt and Pd show broadly positive correlations with MgO, but with significant scatter. Rhenium is positively correlated with  $\text{TiO}_2$  for both islands (Fig. 7; in detail, La Palma and El Hierro define different trends in  $\text{TiO}_2$ –Re space). These relations probably reflect the compatibility of Os,

Ir, Ru, Pt and Pd within early-crystallizing phases (Os, Ir, Ru, Pt, Pd-rich inclusions within chromite, olivine or pyroxene), and the association of Re with late-stage (Fe–Ti oxide) phases. The relative compatibilities of Os, Ir, Ru, Pt, Pd and Re are consistent with those observed for Hawaiian lavas (Ireland et al., 2009). There is also a relationship between decreasing age and MgO content and increasing Re and  $\text{TiO}_2$  for La Palma lavas (Fig. 7): this can be observed both in our dataset and that of Marcantonio et al. (1995). As previously noted, young lavas from the Cumbre Vieja ridge on La Palma often contain amphibole and have different incompatible element inventories compared with Seamount, Taburiente and Garafia lavas. It appears that Re also behaves incompatibly and is elevated in recent Cumbre Vieja lavas.

The  $^{187}\text{Os}/^{188}\text{Os}$  ratios for La Palma lavas range from 0.1378 to 0.1583, with a narrowly constrained average  $^{187}\text{Os}/^{188}\text{Os}$  value of  $0.1459 \pm 0.0049$  ( $2\sigma$ ,  $n = 25$ ). We note that the most extreme isotope compositions occur in basaltic lavas with  $<50$  ppt Os (Fig. 8). Classically, OIB with less than 50 ppt Os have been considered more susceptible

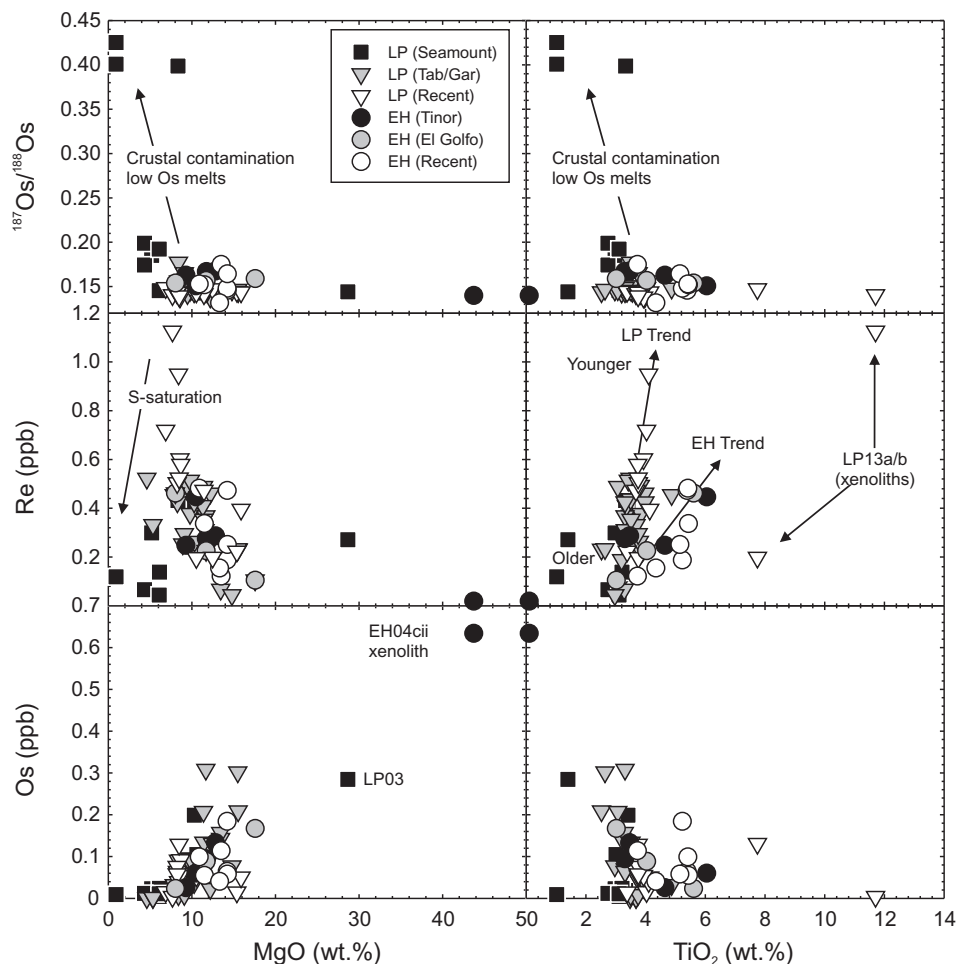


Fig. 7. MgO and  $\text{TiO}_2$  versus Os and Re concentrations and  $^{187}\text{Os}/^{188}\text{Os}$  for El Hierro and La Palma lavas. Positive correlations between Os and MgO, and Re and  $\text{TiO}_2$  indicate that Os behaves compatibly and Re incompatibly, consistent with early-formed phases trapped within olivine controlling Os (as well as Ir, Ru, Pt, Pd), with Re being the most incompatible of the measured HSE. Variation of Re with MgO in seamount pillow lavas (Marcantonio et al., 1995) is consistent with S-saturation, whereas all other lavas are S-undersaturated.

to contamination by high  $^{187}\text{Os}/^{188}\text{Os}$  crustal materials (Reisberg et al., 1993). High Os abundance La Palma samples (>120 ppt) yield a more restricted range in  $^{187}\text{Os}/^{188}\text{Os}$  (0.1421 to 0.1460) and are similar to published values for mafic lavas (>8 wt.% MgO and excluding samples with Os <50 ppt; 0.139 to 0.151; Marcantonio et al., 1995), but do not extend to the radiogenic  $^{187}\text{Os}/^{188}\text{Os}$  ratio of 0.175 published for one sample with 51 ppt Os (LP-4; Widom et al., 1999). Ratios of  $^{187}\text{Os}/^{188}\text{Os}$  in El Hierro lavas range from 0.1387 to 0.1750, greatly extending the previously published range of  $^{187}\text{Os}/^{188}\text{Os}$  measured for 3 El Hierro lavas (0.144 to 0.148; Widom et al., 1999), and yield an average  $^{187}\text{Os}/^{188}\text{Os}$  of  $0.1562 \pm 0.0105$  ( $1\sigma$ ,  $n = 19$ ). High Os El Hierro samples (>120 ppt) yield radiogenic  $^{187}\text{Os}/^{188}\text{Os}$  (0.1481 to 0.1750). All of the samples analysed in this study have supra-chondritic  $\gamma\text{Os}$  (percentage deviation from the time-corrected [in this case essentially present-day] chondritic  $^{187}\text{Os}/^{188}\text{Os}$  reference value; La Palma  $\gamma\text{Os}$  = up to +24.1; El Hierro  $\gamma\text{Os}$  = up to +37.2). El Hierro has the most elevated  $^{187}\text{Os}/^{188}\text{Os}$  recognized for any OIB shield-stage lavas (Fig. 8).

There is limited correlation between  $^{187}\text{Os}/^{188}\text{Os}$  and MgO,  $\text{TiO}_2$ , Ni, modal olivine (Fig. 7; Fig. S7) or  $^{187}\text{Re}/^{188}\text{Os}$  (Fig. S6), although radiogenic  $^{187}\text{Os}/^{188}\text{Os}$  and low Os samples from the La Palma seamount also have low Ni, MgO and  $\text{TiO}_2$  abundances (Marcantonio et al., 1995). One dunite xenolith from El Hierro and 4 clinopyroxene- and/or amphibole-bearing xenoliths from La Palma were analysed for their Re–Os isotope systematics. The El Hierro xenolith has 0.63 ppb Os and  $^{187}\text{Os}/^{188}\text{Os}$  (0.1399) that is considerably lower than for its host lava

(0.1508). Hornblendite and clinopyroxenite xenoliths from La Palma span a range of Os contents (0.004 to 0.131 ppb) and a restricted range of  $^{187}\text{Os}/^{188}\text{Os}$  (0.140 to 0.147).

## 4. DISCUSSION

### 4.1. Crystal–liquid fractionation processes

Volcanic rocks from the Canary Islands span a large compositional range (e.g., Carracedo et al., 2002), reflecting both partial melting and crystal–liquid fractionation processes acting on parental magmas. Clinopyroxenite and hornblendite xenoliths probably represent cumulates generated as by-products of crystal accumulation (e.g., Klügel, 1998; Section S1), and contain amphibole, apatite and free pore space, and  $^{187}\text{Os}/^{188}\text{Os}$  similar to La Palma lavas. Furthermore, cumulate xenoliths and phonolites indicate extensive fractional crystallization recorded in their trace element ratios (e.g., Fig. 3), reflecting crystallization of zircon, feldspar, phosphate and rutile. Ankaramites from La Palma and El Hierro can contain >10% olivine, >15% clinopyroxene and >5% oxides. The compositions of olivine in ankaramites and other lavas span a range of whole-rock Mg#, with a limited maximum forsterite content ( $\sim\text{Fo}_{87}$ ), consistent with accumulation of olivine (Fig. S8). Calculation of olivine and clinopyroxene fractionation indicates up to 30% olivine  $\pm$  clinopyroxene addition and removal from the majority of studied lavas (Fig. 2; Fig. S9). It is well documented that early-formed mineral phases can control the behaviour of Os, Ir and Ru in magmatic rocks (e.g., Barnes et al., 1985) and the HSE patterns of La Palma

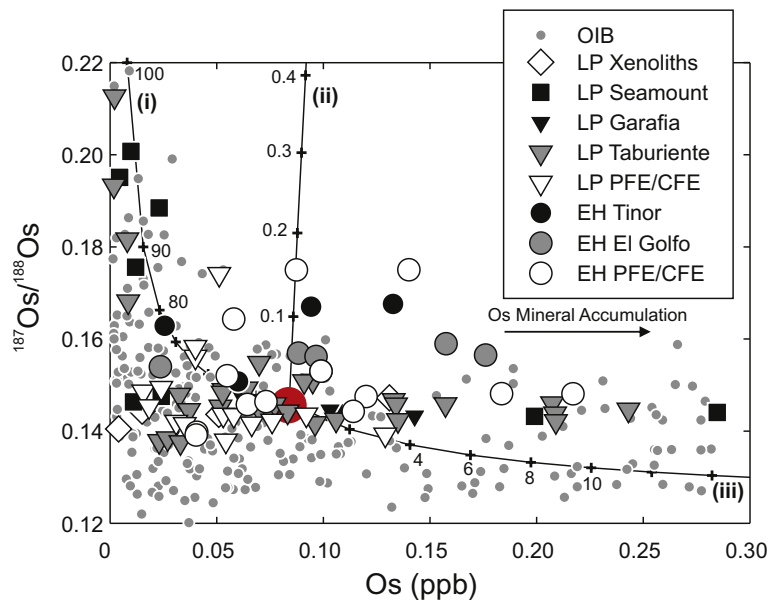


Fig. 8. Whole-rock  $^{187}\text{Os}/^{188}\text{Os}$  versus Os concentrations for La Palma and El Hierro lavas compared with a global OIB dataset. The majority of samples analysed in this study have greater than 50 ppt Os. Also shown are three binary mixing curves (in percent increments) illustrating the effect of assimilation by an average western Canary Island ‘parental melt’ composition (Os = 67 ppt,  $^{187}\text{Os}/^{188}\text{Os}$  = 0.146; see text for details) with: (i) low Os abundance ( $\sim 8$  ppt,  $^{187}\text{Os}/^{188}\text{Os}$  = 0.22) crustal edifice assimilated represented by pillow rind materials (Marcantonio et al., 1995); (ii) high Os abundance Atlantic Fe–Mn crust ( $^{187}\text{Os}/^{188}\text{Os}$  = 1.05; Burton et al., 1999) and (iii) oceanic mantle lithosphere (Os = 1.3 ppb,  $^{187}\text{Os}/^{188}\text{Os}$  = 0.126; Day et al., 2008b; Simon et al., 2008). Global OIB Os dataset from Hauri and Hart (1993), Reisberg et al. (1993), Marcantonio et al. (1995), Lassiter and Hauri (1998), Widom and Shirey (1996), Widom et al. (1999), Eisele et al. (2002), Gaffney et al. (2005), Class et al. (2009), and references therein.

and El Hierro lavas reflect this. Consequently the relationship between MgO versus PGE and Re reflects compatibility (early-formed HSE-rich phases associated with olivine and chromite) of the HSE (Fig. 7).

In addition to shallow-level fractionation, deeper-level (12 to 40 km) clinopyroxene fractionation has been proposed to explain the major element compositions of Iscagua and Fagundo lavas from La Palma (Nikogosian et al., 2002), although this hypothesis has been questioned (Gurenko et al., 2006). Iscagua basanite lavas contain melt inclusions indicating evolved parental melts, and have been interpreted as products of deep-level clinopyroxene fractionation from magma compositions similar to more silica-rich “transitional” Fagundo lavas (Nikogosian et al., 2002). Whole-rocks from Nikogosian et al. (2002) have been measured here for incompatible trace elements,  $^{187}\text{Os}/^{188}\text{Os}$  and HSE abundances to quantify and establish the effect of deeper-level fractionation on these geochemical parameters. No systematic differences are discernable for  $^{187}\text{Os}/^{188}\text{Os}$  or HSE abundances and patterns between Iscagua and Fagundo lavas (Fig. 6b). Therefore, deep-level fractionation has no observable effect on whole-rock HSE abundances compared with shallow-level olivine, clinopyroxene and Cr-spinel fractionation (Fig. 7). Incompatible trace element compositions of Iscagua and Fagundo lavas are also indistinguishable (Table S4). The lack of evidence for deep-level fractionation of clinopyroxene impacting whole-rock geochemistry is indirectly corroborated by Os and Re abundances and  $^{187}\text{Os}/^{188}\text{Os}$  measured in pyroxenite and hornblende cumulate xenoliths (LP13a, LP13b, LP19X, LP21bi) derived from fractional crystallization of parental basaltic magmas.

#### 4.2. Magmatic degassing of rhenium in alkali basalts

Rhenium abundances in sub-aerially erupted tholeiites from Hawai'i are typically lower than submarine equivalents (Bennett et al., 2000; Lassiter, 2003; Ireland et al., 2009). This difference has been explained through magmatic degassing of Re (Bennett et al., 2000; Lassiter, 2003; Norman et al., 2004), or as source characteristics or partial

melting effects (e.g., Hauri and Hart, 1997). Volatile behaviour of Re during eruption is supported by the presence of compounds of this element in volcanic gases (e.g., Crowe et al., 1987; Hinkley et al., 1999). Although Re abundances in alkali basalts have previously been reported, the role magmatic degassing may play in affecting Re concentrations has not been evaluated. Rhenium contents of El Hierro and La Palma lavas are similar to, or lower than Hawai'ian tholeiites of similar MgO content. This is unexpected, since Re is an incompatible element, and should be elevated in lower degree partial melts (Canaries) versus melts from higher degrees of partial melting (Hawai'i). A process other than partial melting must control the Re abundances of alkali and tholeiite OIB. For example, initial source composition, presence of base metal sulphide, oxygen fugacity (sulphide stability; Righter et al., 2008), or Re volatility (Bennett et al., 2000), may all affect magmatic Re abundances.

Alkali basalts tend to have higher concentrations of  $\text{H}_2\text{O}$ ,  $\text{CO}_2$  and the halogens compared with tholeiites (e.g., Hilton et al., 1997), which promotes degassing and loss of volatile elements (Macpherson and Mattey, 1994; Dixon et al., 1995). To assess whether magmatic degassing of Re can explain the variations of this element observed in western Canary Island lavas, we compare Re to La, Cu, Os and Yb (Fig. 9). The rationale for choosing La and Yb is that their partition coefficients for silicate crystal-liquid fractionation are considered to be similar to Re (Hauri and Hart, 1997; Bennett et al., 2000; Norman et al., 2004). Copper, Os and Re are largely controlled by residual sulphide and so are expected to behave similarly during melt transport (Bennett et al., 2000). There is a relationship of decreasing Re/Os, Re/Yb and Re/Cu with decreasing Re abundance for western Canary Island lavas. There is no corresponding evidence for decreasing Cu/Yb, La/Yb or Os/Yb with decreasing Re abundance (Fig. 9). Because Cu contents in Hawai'ian tholeiites (80 to 170 ppm in ~11 wt.% MgO lavas; Norman et al., 2004) are comparable to those of Canary Island lavas of similar MgO contents (70 to 150 ppm), low Re/Cu ratios in the latter reflect lower Re contents than expected in associated parental magmas.

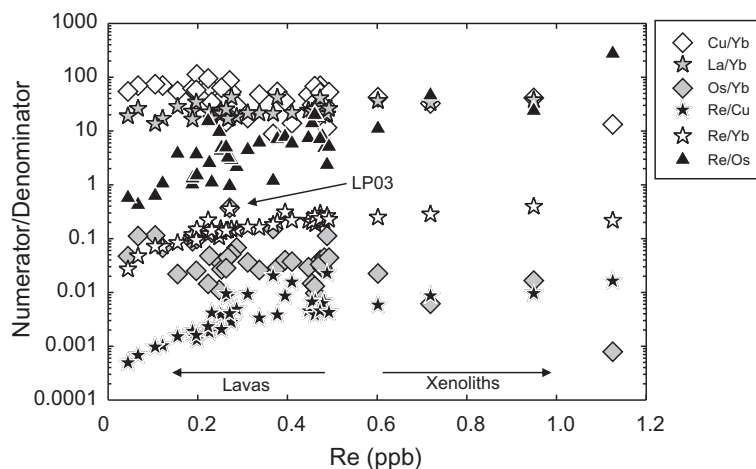


Fig. 9. Ratios of (La, Cu, Os, Re)/Yb, Re/Cu and Re/Os for El Hierro and La Palma lavas.

Lavas with the lowest Re/Yb and Re/Cu are all vesicular and occur in the Taburiente series of La Palma and the young lavas and El Golfo eruptions of El Hierro. The only submarine erupted lava in this study, LP03, has low Re/Cu and the highest Re/Yb of the lavas (Fig. 9).

Oxidized or halogenated complexes of iridium and other HSE can be volatile at basaltic eruption temperatures (>900 °C), where low boiling point (<150 °C) HSE fluoride compounds are generated. For example, Ir has been detected in volcanic aerosols as IrF<sub>6</sub> (Zoller et al., 1983). It is unlikely that Os, Ir, Ru, Pt and Pd show similar volatile behaviour to Re in the present data set. This is because ratios of these elements versus Yb remain constant or slightly increase with decreasing Re abundance (Fig. 9) and because there are strong positive correlations between these elements and indices of fractionation (e.g., MgO; Fig. 7) and modal mineralogy (e.g., olivine; Fig. S9), suggesting sequestration into early-formed trace phases prior to eruption (e.g., Barnes et al., 1985; Ballhaus et al., 2006; Day et al., 2008a). This contrasts with Re, which behaves as a more incompatible element. Therefore, degassing lowers the Re contents in Canary Island lavas, and explain the lack of <sup>187</sup>Re/<sup>188</sup>Os–<sup>187</sup>Os/<sup>188</sup>Os correlations for the lavas (Fig. S6).

#### 4.3. Assimilation processes

Contamination of some Canary Island magmas occurs by interaction with underlying oceanic lithosphere and with edifice materials (e.g., Hoernle and Tilton, 1991; Marcantonio et al., 1995; Thirlwall et al., 1997; Widom et al., 1999; Hilton et al., 2000; Gurenko et al., 2001; Hansteen and Troll, 2003; Lundstrom et al., 2003). Day et al. (2009) have placed limits on the role of assimilation processes for El Hierro and La Palma lavas, and demonstrated the robustness of Os and O isotopes in these rocks to trace mantle processes. Data presented here for oxygen isotopes of fresh olivine and pyroxene pairs confirms this result, with high-temperature equilibrium for nearly all pairs (Fig. S5). Osmium isotopes are sensitive indicators of contamination in OIB because of the contrast of their Os abundances with lithospheric materials (typically >1 ppb Os), and because of their <sup>187</sup>Os/<sup>188</sup>Os compositions (<0.18) relative to crust and sediment (typically <sup>187</sup>Os/<sup>188</sup>Os = >0.4; Reisberg et al., 1991; Marcantonio et al., 1995; Widom et al., 1999), so are used here to further evaluate the potential for crustal or lithospheric assimilation.

Iron–Mn oxide coatings, which are typically characterized by high Os abundances and radiogenic <sup>187</sup>Os/<sup>188</sup>Os compositions, have been suggested as potential assimilants during OIB petrogenesis (e.g., Ireland et al., 2009). We find no evidence for Fe–Mn oxide assimilation, as ~5× greater assimilation would be required to explain <sup>187</sup>Os/<sup>188</sup>Os in El Hierro relative to La Palma lavas, assuming a similar <sup>187</sup>Os/<sup>188</sup>Os starting composition for their parental magmas (Fig. 8; model ii). This would lead to collateral effects with a 20–25% difference in MnO for El Hierro lavas relative to La Palma lavas, which is not observed. The limitation of Fe–Mn oxides as contaminants is clearly demonstrated from low Os abundance (<19 ppt Os) pillow rinds from the La Palma seamount, which show evidence for addition of

radiogenic <sup>187</sup>Os/<sup>188</sup>Os, versus the pillow lava interiors, which do not (Marcantonio et al., 1995).

The oceanic crust beneath the Canary Islands is some of the oldest in the ocean basins (150 to 180 Ma; Hoernle, 1998), and represents a potential contaminant for ascending mantle-derived magmas. Oceanic crust beneath Gran Canaria is composed of an igneous unit (4.5 km thick) overlain by a thick sedimentary apron (up to 6 km). These layers have distinct isotopic compositions and span >50% of <sup>87</sup>Sr/<sup>86</sup>Sr, >60% of <sup>206</sup>Pb/<sup>204</sup>Pb and the full range of δ<sup>18</sup>O compositions measured in OIB (Hoernle, 1998; Hansteen and Troll, 2003; Fig. 4). El Hierro and La Palma samples are correlated in Pb-isotope space and lie along, or are parallel with, the NHRL (Fig. 4). Linearity in multi-isotope space suggests two-component mixing that cannot involve local or pelagic sediment (e.g., Roy-Barman and Allègre, 1995; Thirlwall et al., 1997) as it would force western Canary Island lavas above the NHRL. Jurassic-aged oceanic crust is also too young to account for the range in Sr–Nd–Pb isotope compositions observed for western Canary Island lavas (Thirlwall, 1997; Gurenko et al., 2006).

The observed two-component mixing in Fig. 4 is also unlikely to reflect high-level oceanic crust contamination as bulk mixing between solid crust and melts is highly inefficient and most effective when assimilation is associated with fractional crystallization of the magma (e.g., AFC; DePaolo, 1981). This form of magmatic contamination might result in variations in δ<sup>18</sup>O with indices of differentiation (e.g., Macpherson and Matthey, 1998; Macpherson et al., 2005; Wang and Eiler, 2008), but no such relationship is present in El Hierro or La Palma lavas (Day et al., 2009). Furthermore, unrealistically large quantities of crustal assimilation (~70%; Gurenko et al., 2006) are required assuming the altered portions of underlying oceanic crust to be similar to that sampled beneath Gran Canaria (δ<sup>18</sup>O average = ~4.7‰; <sup>87</sup>Sr/<sup>86</sup>Sr average = ~0.70352; Hoernle, 1998; Hansteen and Troll, 2003).

A final location for potential contamination of magmas is in the underlying oceanic lithospheric mantle (e.g., Widom et al., 1999). However, this form of contamination can be ruled out for El Hierro and La Palma lavas because low Os abundance alkali basalts are highly sensitive to contamination by peridotite. For example, lithospheric mantle xenoliths from Lanzarote are generally Os-rich (>1 ppb) and Re-poor with low <sup>187</sup>Os/<sup>188</sup>Os (<0.126; Day et al., 2008b; Simon et al., 2008). Modeling assimilation of this material (Fig. 8; model iii) shows that contamination by underlying oceanic lithospheric mantle in El Hierro and La Palma lavas is negligible (<1%). In summary, assimilation of crust or lithosphere is unable to account for the geochemical signatures observed in western Canary Island lavas.

#### 4.4. Partial melting and parental melt composition: variable HSE abundances in OIB

Since OIB represent partial melts extracted from the mantle, partial melting and mantle source mineralogy shape their compositions. Primitive Canary Island shield-stage magmas are thought to be picritic (>13 wt.% MgO), derived from >100 km (~30 Kbar; 1500 to 1600 °C) partial melting,

beginning in the garnet stability field (e.g., Schmincke, 1982; Hoernle and Schmincke, 1993). Trace element compositions of western Canary Island lavas are consistent with 2–6% (polybaric) partial melting at 80 to 110 km (Fig. 10; Table S6). Estimated degrees of partial melting are sensitive to melting style (e.g., batch, fractional, etc.), mineral–melt partition co-efficients, melt reaction modes and initial source composition. Nonetheless, estimates of partial melting for El Hierro and La Palma are similar to previous partial melting models for Canary Island lavas (Thirlwall et al., 2000; Carracedo et al., 2002; Gurenko et al., 2006).

Partial melting promotes HSE fractionation (Barnes et al., 1985; Rehkämper et al., 1999), as demonstrated by differences in relative and absolute HSE abundances for high degree partial melts (e.g., most komatiites; *c.f.* Puchtel et al., 2009), versus lower degree equivalents (e.g., MORB; Bézoz et al., 2005). The HSE are primarily controlled by retention of sulphide or Os–Ir–Ru alloy phases in the mantle during partial melting (Ballhaus et al., 2006; Lorand et al., 2010), and by differentiation-related sulphide segregation during magma transport and emplacement (Bézoz

et al., 2005). Osmium, Ir and Ru are dominantly hosted in mono-sulphide solid solution within silicates, or as discrete alloys (Lorand et al., 2010), whereas Pd, Pt and Re are commonly hosted in interstitial sulphide phases (Ballhaus et al., 2006). Consequently, large-degree partial melting may lead to complete sulphur removal in the mantle source and an S-undersaturated melt rich in the HSE (*c.f.*, komatiites), whereas low-degree partial melts (e.g., western Canary Island parental melts) will have variable proportions of HSE resulting from incomplete break-down of sulphide and HSE-rich mantle phases.

The HSE abundances of western Canary Island lavas lie at intermediate concentrations between Hawai'ian lavas (e.g., Ireland et al., 2009) and MORB (Bézoz et al., 2005). Hawai'ian lavas probably derive from 4% to 10% partial melting of their mantle source (Norman and Garcia, 1999) and reflect variable amounts or compositions of residual sulphide during partial melting, with limited differentiation-related sulphide segregation (Bennett et al., 2000). Pacific, Indian and Atlantic MORB glasses probably form from 6 to 16% partial melting of a DMM source, but have suffered sulphide fractionation during magmatic ascent (Bézoz et al., 2005). Like Hawai'ian tholeiites, El Hierro and La Palma lavas derive from an enriched source with respect to DMM (modeled as 'primitive mantle' in Fig. 10), given their elevated and distinct trace element patterns (*c.f.*, Fig. 3). There is negligible fractionation of sulphide in western Canary Island lavas, with Pt and Pd increasing with decreasing MgO (i.e., crystal–liquid fractionation under S-undersaturated conditions). Only low MgO La Palma seamount lavas show strong HSE depletions, implying S-segregation for these melts (Fig. 7).

The lower HSE abundances of La Palma and El Hierro alkali lavas versus Hawai'ian tholeiites supports arguments that the degree of partial melting plays a role in dictating HSE concentrations in derivative melts through incomplete melting of residual sulphide (Rehkämper et al., 1999; Bennett et al., 2000). Fractionation of Pt, Pd and Re from Os, Ir and Ru is evident in western Canary Island lavas from their supra-chondritic Pd/Os, Pt/Os and Re/Os. These ratios are consistent with sulphide retention in the mantle source and sulphur undersaturated melts sourcing El Hierro and La Palma lavas. The HSE abundances of western Canary Island lavas are also consistent with derivation from mantle that is not anomalously enriched or depleted with respect to upper mantle estimates (Becker et al., 2006).

Calculated HSE abundances of parental melts to El Hierro and La Palma lavas are similar, with the notable exception of Pd, and have lower Os, Ir and Ru contents and higher Re/Os ratios than Hawai'ian lavas (Fig. 11; Section S4). Western Canary Island lavas have more elevated Re/Os and  $^{187}\text{Os}/^{188}\text{Os}$  than Hawai'ian lavas, reflecting both lower degrees of partial melting and a more radiogenic Os mantle source. The low Pd/Ir ratios of El Hierro lavas and their parental melt composition relative to lavas from La Palma are probably significant. Petrogenetic processes such as partial melting, crystal–liquid fractionation, crustal assimilation and degassing processes (see above) reveal no obvious method for generating low Pd/Ir in El Hierro lavas. Instead, it is possible that Pd/Ir ratios reflect mantle source

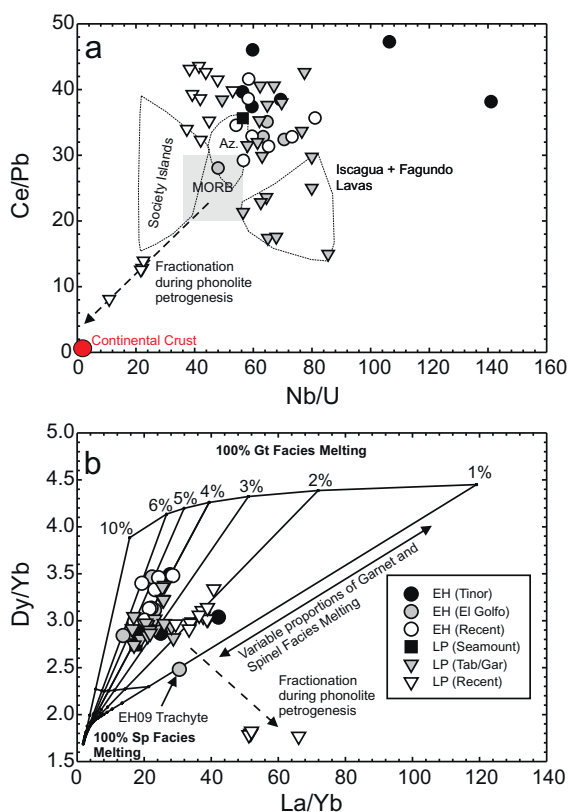


Fig. 10. Plots of: (a) Nb/U versus Ce/Pb and (b) La/Yb versus Dy/Yb. Lavas from El Hierro and La Palma are characterized by elevated Ce/Pb, consistent with HIMU-type OIB (e.g., Hofmann, 2003) and phonolites from La Palma show significant fractionation of incompatible trace element ratios, plotting close to estimates of continental crust in panel a. Iscagua and Fagundo lavas, which are relatively fresh, have low Ce/Pb relative to other El Hierro and La Palma samples, which also coincides with low K contents for Iscagua samples. A partial melt model is shown in panel b, with parameters given in Table S6 for a primitive mantle source.



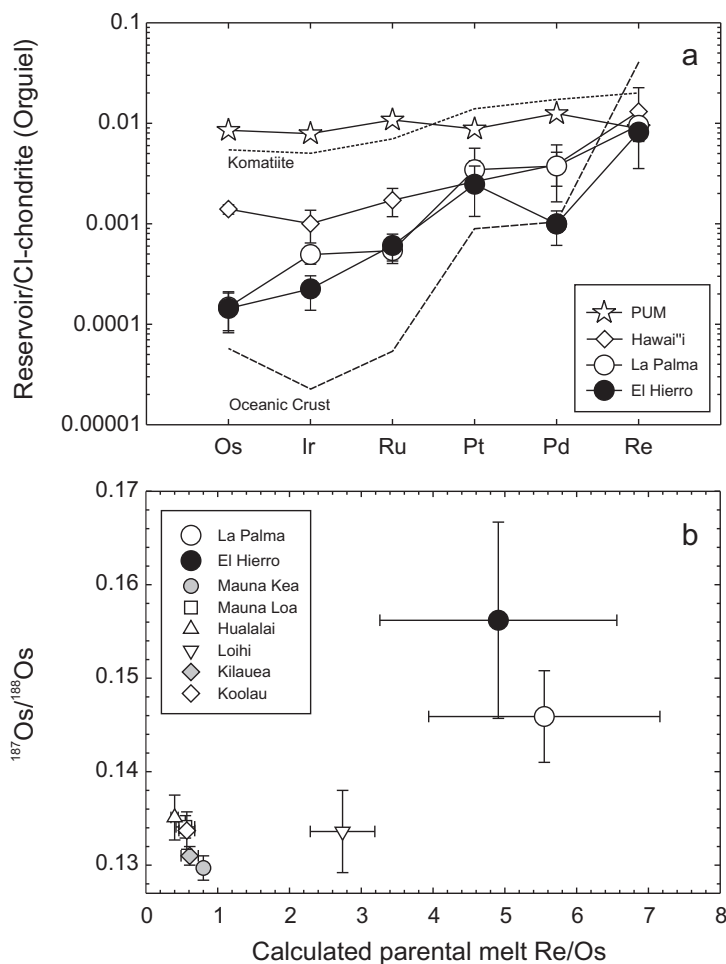


Fig. 11. (a) Chondrite-normalized HSE patterns for estimated parental melt compositions for El Hierro and La Palma. Average parental melt estimate for Hawai'ian picrites (modified after Ireland et al., 2009), primitive upper mantle (PUM; Becker et al., 2006), MORB oceanic crust (Peuker-Ehrinbrink et al., 2003) and a komatiite (Puchtel et al., 2009) are shown for comparison. (b) Calculated parental melt Re/Os ratio versus measured  $^{187}\text{Os}/^{188}\text{Os}$  variations for El Hierro and La Palma, and for Hawai'ian volcanic centers.

characteristics. Some Philippine Sea Plate basalts have low Pd/Ir attributed to a mantle source characteristic (Dale et al., 2008). Low Pd/Ir ratios could be generated during subduction through loss of Pd-rich mineral species (e.g., pentlandite; Dale et al., 2009).

#### 4.5. Identification of distinct portions of recycled crust and lithosphere

The O–Sr–Nd–Os–Pb isotope systematics of western Canary Island lavas represent mixtures of a HIMU-type mantle end-member and a DMM-like component, but lack a third enriched mantle component that is evident in eastern Canary Island lavas (Fig. 4; Sun, 1980; Cousens et al., 1990; Hoernle and Tilton, 1991; Hoernle et al., 1991; Marcantonio et al., 1995; Thirlwall, 1997; Thirlwall et al., 1997; Hoernle, 1998; Widom et al., 1999; Simonsen et al., 2000; Geldmacher et al., 2001; Lundstrom et al., 2003; Geldmacher et al., 2005; Gurenko et al., 2006, 2009; Day et al., 2009). We attribute and identify the HIMU-type end-member in El Hierro and La Palma lavas to distinct

portions of recycled oceanic crust and lithosphere, given: (1) high-TiO<sub>2</sub> contents, which are permissive evidence for a recycled oceanic crust component (Prytulak and Elliott, 2007); (2) depletions in K, Pb, U, Rb, Ba, Cs and Sr relative to water insoluble incompatible elements like Nb, Ta, Zr, Hf and Ti (Fig. 3), which are a predicted consequence of dehydration of subducted oceanic crust (Hofmann and White, 1982; Hofmann et al., 1986; Niu and O'Hara, 2003); (3) estimated parental melt compositions for El Hierro and La Palma which indicate sources with variably high Re/Os, Pt/Os, and  $^{187}\text{Os}/^{188}\text{Os}$ ; (4) low Pd/Ir ratios in El Hierro lavas relative to La Palma lavas, consistent with distinct recycled mantle sources for the two islands; (5) variable and, in the case of La Palma, low  $\delta^{18}\text{O}$  that correlates with radiogenic Os and Pb isotopes; (6) broad correlations between K/U and  $^{206}\text{Pb}/^{204}\text{Pb}$ , as also observed for HIMU-type Raivavae and Rapa lavas (Lassiter et al., 2003; Fig. S11) and; (7) Sr–Nd–Pb–Os isotope compositions consistent with recycled oceanic crust and lithosphere (e.g., Hofmann and White, 1982; Zindler and Hart, 1986; Pegram and Allègre, 1992; Hauri and Hart,

1993; Reisberg et al., 1993; Roy-Barman and Allègre, 1995; Marcantonio et al., 1995; Widom et al., 1999).

Direct melting of ~50–90% of recycled oceanic crust would be required to produce the range of  $^{187}\text{Os}/^{188}\text{Os}$  and  $^{206}\text{Pb}/^{204}\text{Pb}$  observed in OIB (e.g., Becker et al., 2000). This seemingly presents a problem as direct melting of recycled oceanic crust would yield silica-rich, magnesium-poor melts (e.g., Rapp and Watson, 1995; Yaxley and Green, 1998). Alternatively, high-T metasomatised lithospheric mantle has been proposed to explain OIB compositions (Halliday et al., 1995; Niu and O'Hara, 2003; Pilet et al., 2008). Such models cannot explain either the range of O–Os–Pb isotopes in Canary Island lavas without recycled oceanic crust or lithosphere, or low  $\delta^{18}\text{O}$ , since high-T mantle metasomatism has limited effect on O-isotope compositions (Mattey et al., 1994; Chazot et al., 1997).

Mantle peridotite xenoliths typically have bulk  $\delta^{18}\text{O}$  close to MORB estimates (5‰ to 6‰; Mattey et al., 1994; Eiler, 2001), whereas eclogite xenoliths, which are thought to represent fragments of recycled oceanic crust (Garlick et al., 1971), can possess a range of  $\delta^{18}\text{O}$  values ( $\leq 2.5$ ‰ to  $>8$ ‰; Jacob, 2004). It has been suggested that under high-pressures and temperatures in the mantle, recycled eclogite and surrounding peridotite can react to form pyroxenite or hybridized orthopyroxene-rich peridotite with nearly uniform chemical and isotopic composition (Yaxley and Green, 1998; Sobolev et al., 2005, 2007; Spandler et al., 2008). Pyroxenite end-members may locally exhibit significant isotopic variability, however, as observed for Beni Boussera pyroxenites (Pearson and Nowell, 2004). Generation of such hybridized mantle is consistent with the notion of ‘streamline’ mixing of pyroxenite/eclogite and peridotite to form a ‘marble-caked’ mantle (Allègre and Turcotte, 1986). It has further been shown that melting of pyroxenite lithologies can produce silica-undersaturated, iron-rich melts with high-MgO (Hirschmann et al., 2003; Kosigo et al., 2003). Addition of a recycled crustal signature is not restricted to direct melting of pyroxenite in the asthenosphere but may also occur through metasomatic transfer and transplant of melts into the lithosphere (Dasgupta et al., 2006). The lower solidus temperature of pyroxenite versus peridotite leads to greater melt productivity, such that a source with only 1–2% pyroxenite may generate up to 50% of the melt from pyroxenite at low degrees of partial melting (Hirschmann and Stolper, 1996; Hirschmann et al., 2003). Thus, although field evidence indicates pyroxenites are volumetrically minor in the mantle (<1% to 10% e.g., Reisberg et al., 1991; Pearson et al., 1991; Hirschmann et al., 2003), they can contribute extensively to low degree alkalic partial melts (Day et al., 2009; Gurenko et al., 2009), offering an alternative to direct melting of recycled oceanic crust and lithosphere.

#### 4.6. HIMU-peridotite and depleted pyroxenite versus different proportions of oceanic lithosphere?

Numerous models have been proposed to estimate proportions and characteristics of mantle reservoirs contributing to Canary Island magmatism (e.g., Marcantonio et al., 1995; Widom et al., 1999; Day et al., 2009; Gurenko et al.,

2009). There is consensus that the Canary HIMU component differs from ‘classic’ HIMU OIB (St. Helena, Tubuaii, Mangaia; e.g., Thirlwall, 1997). Marcantonio et al. (1995) pointed out the difficulties in matching Os–Pb isotope compositions of La Palma lavas to mixtures between DMM and classic HIMU components. Instead, both Marcantonio et al. (1995) and Widom et al. (1999) have modeled Os–Pb isotope systematics in Canary Island lavas, arriving at mixing between DMM and 15% to 30% of 2 Ga and 25% to 35% of 1.2 Ga recycled oceanic crust, respectively; classic HIMU OIB can be explained by incorporation of 20% to 35% of 1.8 to 2 Ga old recycled oceanic crust.

More complex models have also been proposed to explain isotopic variations observed in the Canary Islands. Widom et al. (1999) suggested mixing between a HIMU-type end-member and a depleted component composed of 50% Palaeozoic (0.5 Ga) recycled oceanic crust and 50% DMM (i.e., a mantle source with two or more distinct recycled components of variable age). This model was expanded by Gurenko et al. (2009), who suggested mixing between HIMU-peridotite mantle and a depleted pyroxenite component. These authors estimated the quantity of pyroxenite and peridotite contributing to lavas and suggested ~70% HIMU-peridotite and ~30% depleted pyroxenite could account for lavas with radiogenic Pb isotopes (e.g., La Palma lavas). For less radiogenic Pb isotope lavas (e.g., El Hierro), Gurenko et al. (2009) estimated ~75% pyroxenite and ~25% peridotite. Finally, Day et al. (2009) demonstrated pronounced O–Os isotope variability between El Hierro and La Palma lavas and explained this through pyroxenite-enriched peridotite mantle containing distinct recycled oceanic lithosphere components. Day et al. (2009) estimated the total pyroxenite component by mass possible in the mantle source and showed that <10% pyroxenite with distinct O–Os isotope characteristics could explain the isotopic variability between the two islands. A corollary here is that the estimates of pyroxenite/peridotite mixing for Canary Island lavas are not mutually exclusive, since the estimated proportions (30% to 75%) of melt generated from pyroxenite, relative to corresponding melt from peridotite (Gurenko et al., 2009), can be from a mantle source with volumetrically minor pyroxenite (<10%; Day et al., 2009).

Using end-member  $^{206}\text{Pb}/^{204}\text{Pb}$  compositions for HIMU-peridotite (20.45) and depleted pyroxenite (Dpx; 19.1), and the quantity of these reservoirs in the source of El Hierro (75% Dpx: 25% HIMU-peridotite) versus La Palma lavas (30% Dpx: 70% HIMU-peridotite) from Gurenko et al. (2009), a mixing model can be generated for the expected Os–O isotope characteristics of this model (Fig. 12). Two major observations can be derived. First, the depleted pyroxenite end-member of Gurenko et al. (2009) is not ‘depleted’ with respect to Re and must have long-term elevated Re/Os (e.g., Fig. 11). Models in Fig. 12 are sensitive to the concentration and isotopic compositions of elements used, but indicate that any depleted pyroxenite reservoir must be more depleted in Os, or enriched in Re, than the HIMU-peridotite end-member. Second, the HIMU-peridotite end-member must have low  $\delta^{18}\text{O}$  (<4.6‰) compared with typical mantle peridotite ( $5.5 \pm 0.2$ ‰, ~5.2‰ in mantle olivines; Mattey et al.,

1994; Eiler, 2001) in addition to having radiogenic  $^{187}\text{Os}/^{188}\text{Os}$  ( $\sim 0.133$ ; Fig. 12; Widom et al., 1999). Given the ubiquitous nature of the HIMU-type component in Canary Island lavas, a necessary implication is that the

HIMU-peridotite reservoir invoked by Gurenko et al. (2009) would be a significant repository of low  $\delta^{18}\text{O}$  in the Canarian mantle. Low  $\delta^{18}\text{O}$  OIB mantle sources have been invoked for the Manus Basin (Macpherson et al.,

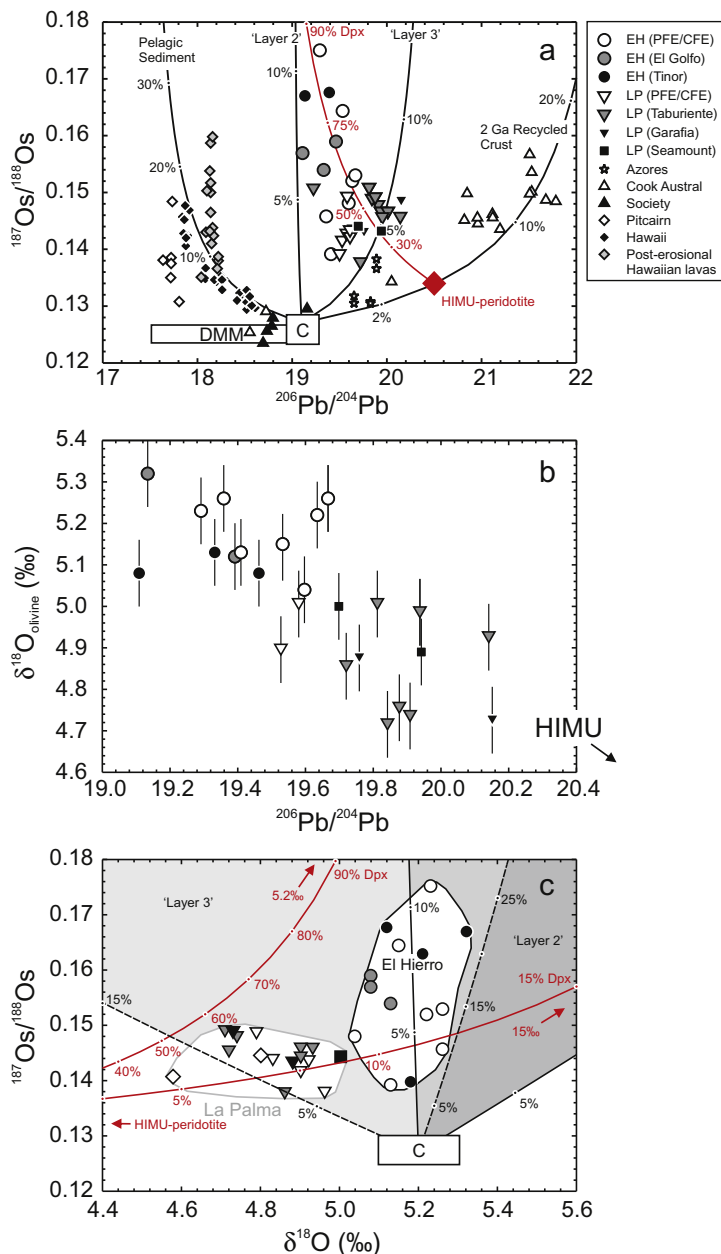


Fig. 12.  $^{206}\text{Pb}/^{204}\text{Pb}$  versus (a)  $^{187}\text{Os}/^{188}\text{Os}$ , and (b)  $\delta^{18}\text{O}$ , and (c)  $\delta^{18}\text{O}$  versus  $^{187}\text{Os}/^{188}\text{Os}$  for El Hierro and La Palma lavas with  $>50$  ppt Os. Shown in (a) is a compilation of global OIB with  $>50$  ppt Os, and mixing curves between a common ('C') mantle component and 2 Ga recycled oceanic crust, pelagic sediment and material conforming to 'Layer-2' and 'Layer-3' recycled oceanic crust and lithosphere. Canary Island lavas can be modeled as mixtures of 'C' and  $<5\%$  to  $10\%$  of HIMU-like pyroxenite-rich mantle with distinct proportions of 'Layer-2' or 'Layer-3' materials (Day et al., 2009), or by generation from mixing between HIMU-peridotite and a 'depleted' pyroxenite (Dpx) component (after Gurenko et al., 2009). Hawai'ian post-erosional lavas can also be explained as pyroxenite-peridotite mixtures (Lassiter et al., 2000). (b) There is a negative trend in  $\delta^{18}\text{O}_{\text{olivine}}$  versus  $^{206}\text{Pb}/^{204}\text{Pb}$  for western Canary Island lavas indicating low  $\delta^{18}\text{O}$  in HIMU mantle ( $1\sigma$  external errors shown for  $\delta^{18}\text{O}_{\text{olivine}}$ ). This relationship is consistent with Sr–Nd–Pb isotope systematics of the lavas (see Fig. S12). O–Os isotope data for western Canary Island lavas (c) can be modeled either as mixtures of pyroxenite with 'Layer-2' ( $5\%$  to  $15\%$ ) and 'Layer-3' ( $0\%$  to  $6\%$ ) like characteristics and 'C', or mixing between HIMU-peridotite and Dpx (after Gurenko et al., 2009). High Os concentrations are estimated for mantle sources from pyroxenites from peridotite massifs (Pearson and Nowell, 2004). Modeling parameters are given in Table S7. Published data from Hauri and Hart (1993), Marcantonio et al. (1995), Widom and Shirey (1996), Hauri (1996), Lassiter and Hauri (1998), Lassiter et al. (2000), Widom et al. (1999), Eisele et al. (2002) and Class et al. (2009). See text for further details.

2000), Iceland (Macpherson et al., 2005), Reykjanes Ridge (Thirlwall et al., 2006), and the Canary Islands (Demeny et al., 2008; Day et al., 2009), but have previously only shown weak correlation, at best, with a HIMU Pb isotope signature (Eiler et al., 1997). Conversely, the depleted pyroxenite component of Gurenko et al. (2009) would require variable  $\delta^{18}\text{O}$  (>5‰ to 15‰) to model the full variation in O–Os isotope space for La Palma and El Hierro lavas (Fig. 12b).

The alternative model is that melts forming the two islands come from different proportions of pyroxenite-rich or refertilised mantle formed by recycled oceanic crust and lithosphere (Day et al., 2009). Mixing trajectories between a ‘common’ component and a recycled basaltic component (assumed to have  $^{187}\text{Os}/^{188}\text{Os}$  and Os concentrations similar to 1.3 Ga Beni Bousera pyroxenite), representing altered ‘Layer-2’ oceanic crust, and a low  $\delta^{18}\text{O}$  recycled gabbro component with elevated U/Pb (HIMU; e.g., Dale et al., 2007) representing ‘Layer-3’ lithosphere are plotted in Fig. 12. To perform model calculations we have assumed that the recycled components are  $\geq 1$  Ga based on the young HIMU affinity of the lavas (Thirlwall, 1997; Widom et al., 1999), otherwise all calculations are identical to those presented in Day et al. (2009) and are provided in Table S7. This model constrains the amount of oceanic crust in the source of both islands to be less than 10% (Day et al., 2009). This model is dependent upon the choice of modeling parameters, most especially O isotope ratios, and it is well established that high-temperature hydrothermal alteration of layer-3 gabbros and peridotites and low-temperature hydrothermal alteration of layer-2 oceanic crust leads to extreme ranges in  $\delta^{18}\text{O}$  (0‰ to 6‰ and 5‰ to 15‰, respectively; Gregory and Taylor, 1981; Alt et al., 1986; Staudigel et al., 1995; Eiler, 2001). A range of oceanic crust and lithosphere O isotope compositions are modeled in Fig. 12, and show that the spectrum of western Canary Island lavas Os–O isotope compositions can be reproduced as mixtures with distinct proportions of recycled crust and lithosphere in their mantle sources.

Both the models of Day et al. (2009) and Gurenko et al. (2009) invoke mixing between a depleted component (DMM) and components refertilised by variable proportions of recycled crust and lithosphere (HIMU), manifested as lithological variations in the mantle sources of Canary Island lavas. Differences are in the details of end-member mixing parameters, but both this study and others (Marcantonio et al., 1995; Widom et al., 1999; Gurenko et al., 2006; Day et al., 2009) offer evidence for mixing between DMM and a mantle reservoir with strong HIMU characteristics in Sr–Nd–Pb isotope space. We also show that the HIMU-type reservoir can have low  $\delta^{18}\text{O}$  and highly variable  $^{187}\text{Os}/^{188}\text{Os}$ , confirming that HIMU can represent a spectrum of compositions (and presumably also mantle lithological variations). These features are consistent with the presence of different proportions of recycled oceanic crust and lithosphere in the source of HIMU-type OIB. Our preferred model, that is supported by the low Pd/Ir ratios of El Hierro lavas, is partial melting of a metasomatised peridotite mantle source containing  $\sim 10\%$  of recycled oceanic lithosphere layer-3 gabbros for La Palma

and layer-2 altered basalt for El Hierro (Day et al., 2009). Maximum age constraints for these reservoirs are <1.8 Ga based on  $^{207}\text{Pb}$ – $^{206}\text{Pb}$  variations for the lavas. This model can explain the distinct arrays observed for O–Sr–Nd–Os–Pb isotopes without the need for complex mixtures of high- $\delta^{18}\text{O}$  Dpx (e.g., Gurenko et al., 2009) to explain the range in Os isotope compositions of El Hierro lavas (Fig. 12). An aspect of our preferred model is that La Palma and El Hierro lavas would represent mixtures of different portions of recycled oceanic crust and lithosphere.

#### 4.7. Implications for OIB and the origin of the HIMU signature

A striking feature of the O–Pb–Os isotope systematics of OIB lavas is the ability to model variations using a common component, marked as ‘C’ in Fig. 12. A common component (C) at the higher end of  $^{187}\text{Os}/^{188}\text{Os}$  measured in DMM samples (abyssal peridotites =  $\sim 0.123$  to  $0.128$ ; e.g., Brandon et al., 2000) is implied by the fact that O–Pb–Os systematics of most OIB require a component that is moderately elevated in  $^{187}\text{Os}/^{188}\text{Os}$ , and that is similar to present-day chondritic  $^{187}\text{Os}/^{188}\text{Os}$  ( $\sim 0.127$ ; Horan et al., 2003), with  $^{206}\text{Pb}/^{204}\text{Pb}$  of  $\sim 19.1$  (Widom et al., 1999; Hauri, 2002). Values of  $\delta^{18}\text{O}$  in the ‘C’ component appear to be close to ‘typical’ mantle values (Day et al., 2009). The ‘C’ component used here is similar to previously postulated FOZO, ‘C’ or PHEM mantle components (Hart et al., 1992; Farley et al., 1992; Hoernle et al., 1995; Hanan and Graham, 1996). Given that OIB define a 1.6 to 2.0 Ga slope in  $^{207}\text{Pb}/^{204}\text{Pb}$ – $^{206}\text{Pb}/^{204}\text{Pb}$  space, representing mixing of the mantle from Archaean to present-day (Hofmann, 2003), these observations support the notion that OIB are not formed via simple mixing between depleted and enriched mantle components, but may sample a mantle that is ‘marble-caked’ (*c.f.*, Allègre and Turcotte, 1986), and has experienced multiple enrichment events from recycled ocean crust and lithosphere. In this scenario, differences in isotopic compositions between OIB and MORB would partly reflect lower degrees of partial melting for OIB, and preferential melting of enriched mantle components, versus large-degrees of decompression melting of DMM and dilution of enriched signatures in the case of MORB. The three major enriched mantle components in OIB (HIMU, EM1, EM2; Zindler and Hart, 1986) would therefore represent recycled materials which are relatively unmixed in the mantle compared with older heterogeneities generated through subduction, which have been more effectively mixed into the mantle (to form the ‘C’, ‘FOZO’, or ‘PHEM’ component(s)).

Another notable feature of modeling O–Os–Pb isotope systematics of OIB is the estimated Os contents of mantle reservoirs. The ‘C’ component and DMM are assumed to have Os concentrations similar to abyssal peridotites ( $\sim 3.3$  ppb; e.g., Marcantonio et al., 1995; Widom et al., 1999). Modeling between a common reservoir and recycled oceanic crust consistently gives unrealistically large quantities of recycled material in the source of OIB to explain their major and trace element compositions (60% to 90% e.g., Becker et al., 2000). However, evidence for radiogenic

( $^{187}\text{Os}/^{188}\text{Os} = 0.126$  to  $0.83$ ), high Os abundance garnet pyroxenites and websterites indicates that pyroxenite-rich peridotite sources may be a reasonable end-member for OIB lavas (Pearson and Nowell, 2004), and would require lower proportions of recycled oceanic crust in their mantle sources (e.g., Fig. 12). More work is required to characterize pyroxenite–peridotite massifs for O–Sr–Nd–Os–Pb isotopes and HSE abundances, but they remain viable analogues for the nature of OIB mantle sources.

Finally, the association of low  $\delta^{18}\text{O}$  with HIMU-type Sr–Nd–Pb signatures and variable and radiogenic  $^{187}\text{Os}/^{188}\text{Os}$  for El Hierro and La Palma lavas constitutes some of the most powerful evidence for recycled crust and lithosphere in the OIB-source mantle. The variable proportions and nature of recycled components required to generate the different isotopic compositions of El Hierro and La Palma lavas provides evidence that the HIMU flavour represents a continuum of compositions and that mantle heterogeneity, even within a single isotopic ‘flavour’, can be preserved in the mantle over the distance of two islands (El Hierro and La Palma are  $\sim 50$  km distant). Furthermore, the preservation of distinct isotopic signatures throughout the accessible stratigraphies of the two islands implies that isotopic heterogeneity is pervasive within their upwelling mantle sources. In addition to a low- $\delta^{18}\text{O}$  HIMU component, a high- $\delta^{18}\text{O}$  HIMU component is also possible in some OIB based on O–Os–Pb isotope systematics.

## 5. CONCLUSIONS

Petrology, whole-rock major- trace- and highly siderophile-element abundances (HSE; Os, Ir, Ru, Pt, Pd, Re) and O–Sr–Nd–Pb–Os isotope systematics are presented for a new suite of lavas and xenoliths from La Palma and El Hierro, Canary Islands. Trace-element data and Sr–Nd–Pb isotope systematics are consistent with HIMU-type mantle sources for the two islands. The most striking aspects of the new dataset are the distinct isotopic differences between El Hierro and La Palma. Broad consistency in isotopic compositions throughout the island stratigraphies implies persistence of isotopic heterogeneities between the islands and throughout their growth. This isotopic variability cannot be explained by crustal contamination processes, however, there is evidence for Re volatility in sub-aerially erupted alkali basalts. It is also shown that crystal–liquid fractionation controls the behaviour of the HSE in the lava suite, but cannot explain the low Pd/Ir in El Hierro relative to La Palma lavas. The HIMU affinity of the two islands in conjunction with the low  $\delta^{18}\text{O}_{\text{olivine}}$  ( $+4.87 \pm 0.18\%$ ;  $^{187}\text{Os}/^{188}\text{Os} = 0.146 \pm 0.005$ ) for La Palma and elevated  $^{187}\text{Os}/^{188}\text{Os}$  for El Hierro lavas ( $0.156 \pm 0.010$ ;  $\delta^{18}\text{O}_{\text{olivine}} = +5.17 \pm 0.08$ ) provides powerful evidence for distinct proportions of recycled oceanic crust and lithosphere beneath the two islands. Direct melting of recycled oceanic crust is unlikely, but reworking of this material is consistent with experimental and field evidence for metasomatised peridotite and pyroxenite formed from oceanic crust and lithosphere. Our preferred model, that is consistent with the geochemical constraints, is partial melting of a metasomatised peridotite mantle source containing  $\sim 10\%$  of recy-

clad oceanic crust and lithosphere as layer-3 gabbros for La Palma and layer-2 altered basalt for El Hierro. The clear isotopic distinction between La Palma and El Hierro lavas strongly supports models of short-length scale ( $\sim 50$  km), long-lived isotopic heterogeneity generated through subduction-related mantle re-enrichment events, and provides powerful evidence for recycled oceanic lithosphere with elevated  $^{206}\text{Pb}/^{204}\text{Pb}$ ,  $^{187}\text{Os}/^{188}\text{Os}$ , and low- $\delta^{18}\text{O}$  in the source of some OIB. Western Canary Island lavas therefore provide further evidence for a heterogeneous mantle sampled by OIB where recycled materials are processed in a similar but distinct manner at different times to generate the spectrum of OIB isotopic compositions.

## ACKNOWLEDGEMENTS

We are grateful to N. Marsh, G.M. Nowell and C.J. Ottley for analytical assistance and T. Elliott for provision of Iscagua and Fagundo lavas. JMDD thanks Pauline Agnew for her help during the 2002 field work campaign. Constructive comments from A. Gurenko, K. Hoernle, M. Jackson and two anonymous reviewers as well as the Associate Editor F. Frey are gratefully acknowledged. This study was conducted as part of a NERC-funded PhD scholarship (NER/S/A/2000/03304) and a *National Geographic Society Research and Exploration* Grant (NGS 8330-07) to JMDD.

## APPENDIX A. SUPPLEMENTARY DATA

Supplementary data associated with this article can be found, in the online version, at doi:10.1016/j.gca.2010.08.021.

## REFERENCES

- Abdel-Monem A., Watkins N. D. and Gast P. W. (1972) Potassium–argon ages, volcanic stratigraphy, and geomagnetic polarity history of the Canary Islands: Tenerife, La Palma and El Hierro. *Am. J. Sci.* **272**, 805–825.
- Allègre C. J. and Turcotte D. L. (1986) Implications of a two-component marble-caked mantle. *Nature* **323**, 123–127.
- Alt J. C., Muehlenbachs K. and Honnorez J. (1986) An oxygen isotopic profile through the upper kilometer of the oceanic crust, DSDP hole 504B. *Earth Planet. Sci. Lett.* **80**, 217–229.
- Ballhaus C., Bockrath C., Wohlgemuth-Ueberwasser C., Laurenz V. and Berndt J. (2006) Fractionation of the noble metals by physical processes. *Contribut. Mineral. Petrol.* **152**, 667–684.
- Barnes S. J., Naldrett A. J. and Gorton M. P. (1985) The origin of the fractionation of platinum-group elements in terrestrial magmas. *Chem. Geol.* **53**, 303–323.
- Bennett V. C., Norman M. D. and Garcia M. O. (2000) Rhenium and platinum-group element abundances correlated with mantle source components in Hawaiian picrites: sulphides in the plume. *Earth Planet. Sci. Lett.* **183**, 513–526.
- Becker H., Jochum K. P. and Carlson R. W. (2000) Trace element fractionation during dehydration of eclogites from high-pressure terranes and the implications for element fluxes in subduction zones. *Chem. Geol.* **163**, 65–99.
- Becker H., Horan M. F., Walker R. J., Gao S., Lorand J.-P. and Rudnick R. L. (2006) Highly siderophile element composition of the Earth’s upper mantle: constraints from new data on peridotite massifs and xenoliths. *Geochim. Cosmochim. Acta* **70**, 4528–4550.

- Bézos A., Lorand J.-P., Humler E. and Gros E. (2005) Platinum-group element systematics in mid-oceanic ridge basalt glasses from the Pacific, Atlantic and Indian oceans. *Geochim. Cosmochim. Acta* **69**, 2613–2627.
- Brandon A. D. and Walker R. J. (2005) The debate over core-mantle interaction. *Earth Planet. Sci. Lett.* **232**, 211–225.
- Brandon A. D., Snow J. E., Walker R. J., Morgan J. W. and Mock T. D. (2000)  $^{190}\text{Pt}$ – $^{186}\text{Os}$  and  $^{187}\text{Re}$ – $^{187}\text{Os}$  systematics of abyssal peridotites. *Earth Planet. Sci. Lett.* **177**, 319–355.
- Burton K. W., Bourdon B., Birck J.-L., Allègre C. J. and Hein J. R. (1999) Osmium isotope variations in the oceans recorded by Fe–Mn crusts. *Earth Planet. Sci. Lett.* **171**, 185–197.
- Carracedo J.-C., Rodríguez Badiola E., Guillou H., De La Nuez J. and Perez Torrado F. J. (2001) Geology and volcanology of La Palma and El Hierro (Canary Islands). *Estudios Geológicos* **57**, 175–273.
- Carracedo J. C., Pérez-Torrado F. J., Ancochea E., Meco J., Hernán F., Cubas C. R., Casillas R., Badiola E. R. and Ahijado A. (2002) Cenozoic volcanism II: the Canary Islands. In *The Geology of Spain* (eds. W. Gibbons and T. Moreno). Geological Society, London, pp. 439–472.
- Chazot G., Lowry D., Menzies M. and Matthey D. (1997) Oxygen isotopic composition of hydrous and anhydrous mantle peridotites. *Geochim. Cosmochim. Acta* **61**, 161–169.
- Class C. and Goldstein S. L. (1997) Plume–lithosphere interactions in the ocean basins: constraints from the source mineralogy. *Earth Planet. Sci. Lett.* **150**, 245–260.
- Class C., Goldstein S. L. and Shirey S. B. (2009) Osmium isotopes in Grand Comore lavas: a new extreme among a spectrum of EM-type mantle endmembers. *Earth Planet. Sci. Lett.* **284**, 219–227.
- Cousens B. L., Spera F. J. and Tilton G. R. (1990) Isotopic patterns in silicic ignimbrites and lava flows of the Mogán and lower Fataga formations, Gran Canaria, Canary Islands: temporal changes in mantle source composition. *Earth Planet. Sci. Lett.* **96**, 319–335.
- Crowe B. M., Finnegan D. L., Zoller W. H. and Boynton W. V. (1987) Trace element geochemistry of volcanic glasses and particles from the 1983–1984 eruptive episodes of Kilauea volcano. *J. Geophys. Res.* **92**, 13708–13714.
- Dale C. W., Gannoun A., Burton K. W., Argles T. W. and Parkinson I. J. (2007) Rhenium–osmium isotope and elemental behaviour during subduction of oceanic crust and implications for mantle recycling. *Earth Planet. Sci. Lett.* **253**, 211–225.
- Dale C. W., Luguet A., Macpherson C. G., Pearson D. G. and Hickey-Vargas R. (2008) Extreme platinum-group element fractionation and variable Os isotope compositions in Philippine Sea Plate basalts: tracing mantle source heterogeneity. *Chem. Geol.* **248**, 213–238.
- Dale C. W., Burton K. W., Pearson D. G., Gannoun A., Alard O., Argles T. W. and Parkinson I. J. (2009) Highly siderophile element behaviour accompanying subduction of oceanic crust: whole rock and mineral-scale insights from a high-pressure terrain. *Geochim. Cosmochim. Acta* **73**, 1394–1416.
- Dasgupta R., Hirschmann M. M. and Stalker K. (2006) Immiscible transition from carbonate-rich to silicate-rich melts in the 3 GPa melting interval of eclogite +  $\text{CO}_2$  and genesis of silica-undersaturated ocean island lavas. *J. Petrol.* **47**, 647–671.
- Day J. M. D., Pearson D. G. and Hulbert L. J. (2008a) Rhenium–osmium isotope and platinum-group element constraints on the origin and evolution of the 1.27 Ga Muskox Intrusion. *J. Petrol.* **49**, 1255–1295.
- Day J. M. D., Walker R. J., Hilton D. R., Carracedo J.-C. and Hanski E. (2008b) Constraining deep mantle contributions to Canary Island lavas. *Geochim. Cosmochim. Acta* **72**, A204.
- Day J. M. D., Pearson D. G., Macpherson C. G., Lowry D. and Carracedo J.-C. (2009) Pyroxenite-rich mantle formed by recycled oceanic lithosphere: oxygen–osmium isotope evidence from Canary Island lavas. *Geology* **37**, 555–558.
- Demeny A., Cassillas R., Vennemann T. W., Hegner E., Nagy G., Ahijado A., De La Nuez J., Sipos P., Pilet S. and Milton J. (2008) Plume-related stable isotope compositions and fluid–rock interaction processes in the Basal Complex of La Palma, Canary Islands, Spain. In *Metasomatism in Oceanic and Continental Lithospheric Mantle*, vol. 293 (eds. M. Coltorti and M. Grecco). Geological Society, London, Special Publications, pp. 155–175.
- DePaolo D. J. (1981) Trace element and isotopic effects of combined wallrock assimilation and fractional crystallisation. *Earth Planet. Sci. Lett.* **53**, 189–202.
- Dixon J. E., Stolper E. M. and Holloway J. R. (1995) An experimental study of water and carbon dioxide solubilities in mid-ocean ridge basaltic liquids. Part I: calibration and solubility models. *J. Petrol.* **36**, 1607–1631.
- Eiler J. M. (2001) Oxygen isotope variations of basaltic lavas and upper mantle rocks. *Rev. Mineral. Geochem.* **43**, 319–364.
- Eiler J. M., Farley K. A., Valley J. W., Hoffman A. W. and Stolper E. M. (1996) Oxygen isotope constraints on the sources of Hawaiian volcanism. *Earth Planet. Sci. Lett.* **144**, 453–468.
- Eiler J. M., Farley K. A., Valley J. W., Hauri E., Craig H., Hart S. R. and Stolper E. M. (1997) Oxygen isotope variations in ocean island basalt phenocrysts. *Geochim. Cosmochim. Acta* **61**, 2281–2293.
- Eiler J. M., Schiano P., Kitchen N. and Stolper E. M. (2000) Oxygen-isotope evidence for recycled crust in the sources of mid-ocean-ridge basalts. *Nature* **403**, 530–534.
- Eisele K., Sharma M., Galer S. J. G., Blichert-Toft J., Devey C. W. and Hofmann A. W. (2002) The role of sediment recycling in EM-1 inferred from Os, Pb, Hf, Nd, Sr isotope and trace element systematics of the Pitcairn hotspot. *Earth Planet. Sci. Lett.* **196**, 197–212.
- Elliott T., Blichert-Toft J., Heumann A., Koetsier G. and Forjaz V. (2007) The origin of enriched mantle beneath São Miguel, Azores. *Geochim. Cosmochim. Acta* **71**, 219–240.
- Farley K. A., Natland J. H. and Craig H. (1992) Binary mixing of enriched and undegassed (primitive?) mantle components (He, Sr, Nd, Pb) in Samoan lavas. *Earth Planet. Sci. Lett.* **111**, 183–199.
- Gaffney A. M., Nelson B. K., Reisberg L. and Eiler J. (2005) Oxygen–osmium isotope systematics of West Maui lavas: a record of shallow-level magmatic processes. *Earth Planet. Sci. Lett.* **239**, 122–139.
- Gannoun A., Burton K. W., Parkinson I. J., Alard O., Schiano P. and Thomas L. E. (2007) The scale and origin of the osmium isotope variations in mid-ocean ridge basalts. *Earth Planet. Sci. Lett.* **259**, 541–556.
- García M. O., Ito E., Eiler J. M. and Pietruszka A. J. (1998) Crustal contamination of Kilauea volcano magmas revealed by oxygen isotope analyses of glass and olivine from Puu’Oo eruption lavas. *J. Petrol.* **39**, 803–817.
- García M. O., Ito E. and Eiler J. M. (2008) Oxygen isotope evidence for chemical interaction of Kilauea historical magmas with basement rocks. *J. Petrol.* **49**, 757–769.
- Gast P. W., Tilton G. R. and Hedge C. (1964) Isotopic composition of lead and strontium from Ascension and Gough Islands. *Science* **145**, 1181–1185.
- Garlick G. D., Macgregor I. D. and Vogel D. E. (1971) Oxygen isotope ratios in eclogites from kimberlites. *Science* **172**, 1025–1027.
- Geldmacher J., Hoernle K., van den Bogaard P., Zankl G. and Garbe-Schönberg D. (2001) Earlier history of the 70-Ma-old

- Canary hotspot based on the temporal and geochemical evolution of the Selvagen archipelago and neighbouring seamounts in the eastern North Atlantic. *J. Volcanol. Geotherm. Res.* **111**, 55–87.
- Geldmacher J., Hoernle K., Bogaard P. v. d., Duggen S. and Werner R. (2005) New  $^{40}\text{Ar}/^{39}\text{Ar}$  age and geochemical data from seamounts in the Canary and Madeira volcanic provinces: support for the mantle plume hypothesis. *Earth Planet. Sci. Lett.* **237**, 85–101.
- Graham D. W., Humphris S. E., Jenkins W. J. and Kurz M. D. (1992) Helium isotope geochemistry of some volcanic rocks from Saint Helena. *Earth Planet. Sci. Lett.* **110**, 121–131.
- Gregory R. T. and Taylor H. P. (1981) An oxygen isotope profile in a section of Cretaceous oceanic crust, Samail ophiolite, Oman: evidence for  $\delta^{18}\text{O}$  buffering of the oceanic by deep (>5 km) seawater-hydrothermal circulation at mid-ocean ridges. *J. Geophys. Res.* **86**, 2737–2755.
- Guillou H., Carracedo J.-C., Pérez Torrado F. and Badiola E. R. (1996) K–Ar ages and magnetic stratigraphy of a hotspot-induced, fast grown oceanic island: El Hierro, Canary Islands. *J. Volcanol. Geotherm. Res.* **73**, 141–155.
- Guillou H., Carracedo J.-C. and Day S. J. (1998) Dating of the Upper Pleistocene–Holocene volcanic activity of La Palma using the unspiked K–Ar technique. *J. Volcanol. Geotherm. Res.* **86**, 137–149.
- Gurenko A. A., Chaussidon M. and Schmincke H.-U. (2001) Magma ascent and contamination beneath one intraplate volcano: evidence from S and O isotopes in glass inclusions and their host clinopyroxenes from Miocene basaltic hyaloclastites southwest of Gran Canaria (Canary Islands). *Geochim. Cosmochim. Acta* **65**, 4359–4374.
- Gurenko A. A., Hoernle K. A., Hauff F., Schmincke H.-U., Han D., Miura Y. N. and Kaneoka I. (2006) Major, trace element and Nd–Sr–Pb–O–He–Ar isotope signatures of shield stage lavas from the central and western Canary Islands: insights into mantle and crustal processes. *Chem. Geol.* **233**, 75–112.
- Gurenko A. A., Sobolev A. V., Hoernle K. A., Hauff F. and Schmincke H.-U. (2009) Enriched, HIMU-type peridotite and depleted recycled pyroxenite in the Canary plume: a mixed-up mantle. *Earth Planet. Sci. Lett.* **277**, 514–524.
- Halliday A. N., Lee D.-C., Tommasini S., Davies G. R., Paslick C. R., Fitton J. G. and James D. E. (1995) Incompatible trace elements in OIB and MORB and source enrichment in the sub-oceanic mantle. *Earth Planet. Sci. Lett.* **133**, 379–395.
- Hanan B. B. and Graham D. W. (1996) Lead and helium isotope evidence from oceanic basalts for a common deep source of mantle plumes. *Science* **272**, 991–995.
- Hansteen T. H. and Troll V. R. (2003) Oxygen isotope composition of xenoliths from the oceanic crust and volcanic edifice beneath Gran Canaria (Canary Islands): consequences for crustal contamination of ascending magmas. *Chem. Geol.* **193**, 181–193.
- Hart S. R. (1984) A large-scale isotope anomaly in the southern hemisphere mantle. *Nature* **309**, 753–757.
- Hart S. R., Hauri E. H., Oschmann L. A. and Whitehead J. A. (1992) Mantle plumes and entrainment: isotopic evidence. *Science* **256**, 517–520.
- Hauri E. H. (1996) Major element variability in the Hawaiian mantle plume. *Nature* **382**, 415–419.
- Hauri E. H. (2002) Osmium isotopes and mantle convection. *Philos. Trans. Royal Soc. London, A* **360**, 2371–2382.
- Hauri E. H. and Hart S. R. (1993) Re–Os isotope systematics of HIMU and EMII oceanic island basalts from the South Pacific Ocean. *Earth Planet. Sci. Lett.* **114**, 353–371.
- Hauri E. H. and Hart S. R. (1997) Rhenium abundances and systematics in oceanic basalts. *Chem. Geol.* **139**, 185–205.
- Hernandéz-Pacheco A. and Valls M. C. (1982) The historic eruptions of La Palma Island (Canarias). *Arquipelago, Rev. Univ. Azores Ser. C. Nat.* **3**, 83–94.
- Hilton D. R., McMurtry G. M. and Kreulen R. (1997) Large variations in vent fluid  $\text{CO}_2/{}^3\text{He}$  ratios signal rapid changes in magma chemistry at Loihi seamount, Hawaii. *Nature* **396**, 359–362.
- Hilton D. R., Macpherson C. G. and Elliot T. R. (2000) Helium isotope ratios in HIMU lavas and geothermal fluids from La Palma, the Canary Islands (Spain): implications for HIMU mantle sources. *Geochim. Cosmochim. Acta* **64**, 2119–2132.
- Hinkley T. K., Lamothe P. J., Wilson S. A., Finnegan D. L. and Gerlach T. M. (1999) Metal emissions at Kilauea and a suggested revision of the estimated worldwide metal output by quiescent degassing volcanoes. *Earth Planet. Sci. Lett.* **170**, 315–325.
- Hirschmann M. M. and Stolper E. M. (1996) A possible role for garnet pyroxenite in the origin of the “garnet signature” in MORB. *Contrib. Mineral. Petrol.* **124**, 185–208.
- Hirschmann M. M., Kosigo T., Baker M. B. and Stolper E. M. (2003) Alkalic magmas generated by partial melting of garnet pyroxenite. *Geology* **31**, 481–484.
- Hoernle K. (1998) Geochemistry of Jurassic oceanic crust beneath Gran Canaria (Canary Islands): implications for crustal recycling and assimilation. *J. Petrol.* **39**, 859–880.
- Hoernle K. and Tilton G. (1991) Sr–Nd–Pb isotope data for Fuerteventura (Canary Islands) basal complex and subaerial volcanics: application to magma genesis and evolution. *Schweizerische Mineralogische und Petrographische Mitteilungen* **71**, 5–21.
- Hoernle K. and Schmincke H.-U. (1993) The role of partial melting in the 15-Ma geochemical evolution of Gran Canaria: a blob model for the Canary hotspot. *J. Petrol.* **34**, 599–626.
- Hoernle K., Tilton G. and Schmincke H.-U. (1991) Sr–Nd–Pb isotopic evolution of Gran Canaria: evidence for shallow enriched mantle beneath the Canary Islands. *Earth Planet. Sci. Lett.* **106**, 44–63.
- Hoernle K. A., Zhang Y.-S. and Graham D. W. (1995) Seismic and geochemical evidence for large-scale mantle upwelling beneath the eastern Atlantic and western and central Europe. *Nature* **374**, 34–39.
- Hofmann A. W. (1997) Mantle geochemistry: the message from oceanic volcanism. *Nature* **385**, 219–229.
- Hofmann A. W. (2003) Sampling mantle heterogeneity through oceanic basalts: isotopes and trace elements. In *The Mantle*, vol. 2 (ed. R. W. Carlson), *Treatise on Geochemistry* (eds. H. D. Holland and K. K. Turekian), Elsevier–Pergamon, Oxford. pp. 61–101.
- Hofmann A. W. and White W. M. (1982) Mantle plumes from ancient oceanic crust. *Earth Planet. Sci. Lett.* **57**, 421–436.
- Hofmann A. W., Jochum K. P., Seufert M. and White W. M. (1986) Nb and Pb in oceanic basalts: new constraints on mantle evolution. *Earth Planet. Sci. Lett.* **79**, 33–45.
- Horan M., Walker R. J., Morgan J. W., Grossman J. N. and Rubin A. E. (2003) Highly siderophile elements in chondrites. *Chem. Geol.* **196**, 5–20.
- Ireland T. J., Walker R. J. and Garcia M. O. (2009) Highly siderophile element and  $^{187}\text{Os}$  isotope systematics of Hawaiian picrites: implications for parental melt composition and source heterogeneity. *Chem. Geol.* **260**, 112–128.
- Jacob D. (2004) Nature and origin of eclogite xenoliths from kimberlites. *Lithos* **77**, 295–316.
- Klügel A. (1998) Reactions between mantle xenoliths and host magma beneath La Palma (Canary Islands): constraints on magma ascent rates and crustal reservoirs. *Contrib. Mineral. Petrol.* **131**, 237–257.

- Klügel A., Hoernle K., Schmincke H.-U. and White J. D. L. (2000) The chemically zoned 1949 eruption on La Palma (Canary Islands): petrological evolution and magma supply dynamics of a rift zone eruption. *J. Geophys. Res.* **105**, 5997–6016.
- Kosigo T., Hirschmann M. M. and Frost D. J. (2003) High-pressure partial melting of garnet pyroxenite: possible mafic lithologies in the source of ocean island basalts. *Earth Planet. Sci. Lett.* **216**, 603–617.
- Lassiter J. C. (2003) Rhenium volatility in subaerial lavas: constraints from subaerial and submarine portions of the HSDP-2 Mauna Kea drill core. *Earth Planet. Sci. Lett.* **214**, 311–325.
- Lassiter J. C. and Hauri E. H. (1998) Osmium-isotope variations in Hawaiian lavas: evidence for recycled oceanic lithosphere in the Hawaiian plume. *Earth Planet. Sci. Lett.* **164**, 483–496.
- Lassiter J. C., Hauri E. H., Reiners P. W. and Garcia M. O. (2000) Generation of Hawaiian post-erosional lavas by melting of a mixed lherzolite/pyroxenite source. *Earth Planet. Sci. Lett.* **178**, 269–284.
- Lassiter J. C., Blichert-Toft J., Hauri E. H. and Barseczus H. G. (2003) Isotope and trace element variations in lavas from Raivavae and Rapa, Cook-Austral Islands: constraints on the nature of HIMU- and EM-mantle and the origin of mid-plate volcanism in French Polynesia. *Chem. Geol.* **202**, 115–138.
- Lorand J.-P., Alard O. and Luguet A. (2010) Platinum-group element micronuggets and refertilization process in Lherz orogenic massif (northeastern Pyrenees, France). *Earth Planet. Sci. Lett.* **289**, 298–310.
- Lowry D., Appel P. W. U. and Rollinson H. R. (2003) Oxygen isotopes of an early Archaean layered ultramafic body, southern West Greenland: implications for magma source and post-intrusion history. *Precamb. Res.* **126**, 273–288.
- Lundstrom C. C., Hoernle K. and Gill J. (2003) U-series disequilibria in volcanic rocks from the Canary Islands: plume versus lithospheric melting. *Geochim. Cosmochim. Acta* **67**, 4153–4177.
- Macpherson C. and Matthey D. P. (1994) Carbon isotope variations of CO<sub>2</sub> in Central Lau Basin basalts and ferrobasalts. *Earth Planet. Sci. Lett.* **121**, 263–276.
- Macpherson C. G. and Matthey D. P. (1998) Oxygen isotope variations in Lau Basin lavas. *Chem. Geol.* **144**, 177–194.
- Macpherson C. G., Hilton D. R., Matthey D. P. and Sinton J. M. (2000) Evidence for an <sup>18</sup>O-depleted mantle plume from contrasting <sup>18</sup>O/<sup>16</sup>O ratios of back-arc lavas from the Manus Basin and Mariana Trough. *Earth Planet. Sci. Lett.* **176**, 171–183.
- Macpherson C. G., Hilton D. R., Day J. M. D., Lowry D. and Grönvold K. (2005) High-<sup>3</sup>He/<sup>4</sup>He depleted mantle and low-<sup>δ</sup><sup>18</sup>O recycled oceanic lithosphere in the source of central Icelandic lavas. *Earth Planet. Sci. Lett.* **233**, 411–427.
- Malamud B. D. and Turcotte D. L. (1999) How many plumes are there? *Earth Planet. Sci. Lett.* **174**, 113–124.
- Marcantonio F., Zindler A., Elliott T. and Staudigel H. (1995) Os isotope systematics of La Palma, Canary Islands: evidence for recycled crust in the mantle source of HIMU ocean islands. *Earth Planet. Sci. Lett.* **133**, 397–410.
- Matthey D. P., Lowry D. and Macpherson C. (1994) Oxygen isotope composition of mantle peridotite. *Earth Planet. Sci. Lett.* **128**, 231–241.
- McDonough W. F. and Sun S.-s. (1995) The composition of the Earth. *Chem. Geol.* **120**, 223–253.
- Morgan W. J. (1981) Hotspot tracks and the opening of the Atlantic and Indian oceans. In *The Sea* (ed. C. Emiliani). John Wiley, New York.
- Nikogosian I. K., Elliott T. and Touret J. L. R. (2002) Melt evolution beneath thick lithosphere: a magmatic inclusion study of La Palma, Canary Islands. *Chem. Geol.* **183**, 169–193.
- Niu Y. and O'Hara M. J. (2003) Origin of ocean island basalts: a new perspective from petrology, geochemistry and mineral physics considerations. *J. Geophys. Res.* **108**. doi:10.1029/2002JB002048.
- Norman M. D. and Garcia M. O. (1999) Primitive magmas and source characteristics of the Hawaiian plume: petrology and geochemistry of shield picrites. *Earth Planet. Sci. Lett.* **168**, 27–44.
- Norman M. D., Garcia M. O. and Bennett V. C. (2004) Rhenium and chalcophile elements in basaltic glasses from Ko'olau and Moloka'i volcanoes: magmatic outgassing and composition of the Hawaiian plume. *Geochim. Cosmochim. Acta* **68**, 3761–3777.
- O'Hara M. J. (1996) Volcanic plumbing and the space problem-thermal and geochemical consequences of large-scale assimilation in ocean island development. *J. Petrol.* **39**, 1077–1089.
- Paris R., Guillou H., Carracedo J.-C. and Pérez Torrado F. J. (2005) Volcanic and morphological evolution of La Gomera (Canary Islands), based on new K/Ar ages and magnetic stratigraphy: implications for oceanic island evolution. *J. Geol. Soc., London* **162**, 501–512.
- Pearson D. G. and Nowell G. M. (2004) Re–Os and Lu–Hf isotopic constraints on the origin and age of pyroxenites from the Beni Bousera peridotite massif: implications for mixed peridotite–pyroxenite mantle sources. *J. Petrol.* **45**, 439–455.
- Pearson D. G., Davies G. R., Nixon P. H., Greenwood P. B. and Matthey D. P. (1991) Oxygen isotope evidence for the origin of pyroxenites in the Beni Bousera peridotite massif N. Morocco: derivation from subducted oceanic lithosphere. *Earth Planet. Sci. Lett.* **102**, 289–301.
- Pegram W. J. and Allègre C. J. (1992) Osmium isotopic compositions from oceanic basalts. *Earth Planet. Sci. Lett.* **111**, 59–68.
- Peuker-Ehrinbrink B., Bach W., Hart S. R., Blusztajn J. S. and Abbruzzese T. (2003) Rhenium–osmium isotope systematics and platinum group element concentrations in oceanic crust from DSDP/ODP sites 504 and 417/418. *Geochem., Geophys., Geosyst.* **4**, 1–28.
- Pilet S., Baker M. B. and Stolper E. M. (2008) Metasomatized lithosphere and the origin of alkaline lavas. *Science* **320**, 916–919.
- Prytulak J. and Elliott T. (2007) TiO<sub>2</sub> enrichment in ocean island basalts. *Earth Planet. Sci. Lett.* **263**, 388–403.
- Puchtel I. S., Walker R. J., Brandon A. D. and Nisbet E. G. (2009) Pt–Re–Os and Sm–Nd isotope and HSE and REE systematics of the 2.7 Ga Belingwe and Abitibi komatiites. *Geochim. Cosmochim. Acta* **73**, 6367–6389.
- Rapp R. P. and Watson E. B. (1995) Dehydration melting of metabasalt at 8–32 kbar: implications for continental growth and crust–mantle recycling. *J. Petrol.* **36**, 891–931.
- Rehkämper M. and Hofmann A. W. (1997) Recycled oceanic crust and sediment in Indian Ocean MORB. *Earth Planet. Sci. Lett.* **147**, 93–106.
- Rehkämper M., Halliday A. N., Fitton J. G., Lee D.-C., Wieneke M. and Arndt N. T. (1999) Ir, Ru, Pt and Pd in basalts and komatiites: new constraints for the geochemical behaviour of the platinum-group elements in the mantle. *Geochim. Cosmochim. Acta* **63**, 3915–3934.
- Reisberg L., Allègre C. J. and Luck J.-M. (1991) The Re–Os systematics of the Ronda ultramafic complex of Southern Spain. *Earth Planet. Sci. Lett.* **105**, 196–213.
- Reisberg L., Zindler A., Marcantonio F., White W., Wyman D. and Weaver B. (1993) Os isotope systematics in ocean island basalts. *Earth Planet. Sci. Lett.* **120**, 149–167.
- Righter K., Chesley J. T., Caiazza C. M., Gibson E. K. and Ruiz J. (2008) Re and Os concentrations in arc basalts: the roles of volatility and source region fO<sub>2</sub> variations. *Geochim. Cosmochim. Acta* **72**, 926–947.



- Roy-Barman M. and Allègre C. J. (1995)  $^{187}\text{Os}/^{186}\text{Os}$  in oceanic island basalts: tracing oceanic crust recycling in the mantle. *Earth Planet. Sci. Lett.* **129**, 145–161.
- Rudnick R. L. and Gao S. (2003) Composition of the continental crust. In *The Crust*, vol. 3 (ed. R. L. Rudnick), *Treatise on Geochemistry* (eds. H. D. Holland and K. K. Turekian), Elsevier–Pergamon, Oxford. pp. 1–64.
- Schmincke H.-U. (1982) Volcanic and chemical evolution of the Canary Islands. In *Geology of the Northwest African Continental Margin* (eds. U. von Rad, K. Hinz, M. Sarnthein and E. Seibold). Springer, pp. 273–306.
- Simon N. S. C., Neumann E.-R., Bonadiman C., Coltorti M., Delpech G., Grégoire M. and Widom E. (2008) Ultra-refractory domains in the oceanic lithosphere sampled as mantle xenoliths in ocean islands. *J. Petrol.* **49**, 1223–1251.
- Simonsen S. L., Neumann E.-R. and Siem K. (2000) Sr–Nd–Pb isotope and trace-element geochemistry evidence for a young HIMU source and assimilation at Tenerife (Canary Island). *J. Volcanol. Geotherm. Res.* **103**, 299–312.
- Sobolev A. V., Hofmann A. W., Sobolev S. V. and Nikogosian I. K. (2005) An olivine-free mantle source of Hawaiian shield basalts. *Nature* **434**, 590–597.
- Sobolev A. V. 19 authors (2007) The amount of recycled crust in sources of mantle-derived melts. *Science* **316**, 412–417.
- Spandler C., Yaxley G., Green D. H. and Rosenthal A. (2008) Phase relations and melting of anhydrous K-bearing eclogite from 1200 to 1600 °C and 3 to 5 GPa. *J. Petrol.* **49**, 771–795.
- Staudigel H., Davies G. R., Hart S. R., Marchant K. M. and Smith B. M. (1995) Large-scale isotopic Sr, Nd and O isotopic anatomy of altered oceanic crust-DSDP/ODP sites 417/418. *Earth Planet. Sci. Lett.* **130**, 169–185.
- Sun S.-s. (1980) Lead isotopic study of young volcanic rocks from mid-ocean ridges, ocean islands and island arcs. In *The Evidence for Chemical Heterogeneity in Earth's Mantle* (eds. K. Bailey, J. Tarney and K. Dunham). Royal Society of London, pp. 409–445.
- Thirlwall M. F. (1997) Pb isotopic and elemental evidence for OIB derivation from young HIMU mantle. *Chem. Geol.* **139**, 51–74.
- Thirlwall M. F., Jenkins C., Vroon P. Z. and Matthey D. P. (1997) Crustal interaction during construction of ocean islands: Pb–Sr–Nd–O isotope geochemistry of the shield basalts of Gran Canaria, Canary Islands. *Chem. Geol.* **135**, 233–262.
- Thirlwall M. F., Singer B. F. and Marriner G. F. (2000)  $^{39}\text{Ar}$ – $^{40}\text{Ar}$  ages and geochemistry of the basaltic shield stage of Tenerife, Canary Islands, Spain. *J. Volcanol. Geotherm. Res.* **103**, 247–297.
- Thirlwall M. F., Gee M. A. M., Lowry D., Matthey D. P., Murton B. J. and Taylor R. N. (2006) Low  $\delta^{18}\text{O}$  in the Icelandic mantle and its origins: Evidence from Reykjanes Ridge and Icelandic lavas. *Geochim. Cosmochim. Acta* **70**, 993–1019.
- Wang Z. and Eiler J. M. (2008) Insights into the origin of low- $\delta^{18}\text{O}$  basaltic magmas in Hawaii revealed from in situ measurements of oxygen isotope compositions of olivines. *Earth Planet. Sci. Lett.* **269**, 377–387.
- White W. M. (1985) Source of oceanic basalts: radiogenic isotope evidence. *Geology* **13**, 115–118.
- Whitehouse M. J. and Neumann E.-R. (1995) Sr–Nd–Pb isotope data for ultramafic xenoliths from Hierro, Canary Islands: melt infiltration processes in the upper mantle. *Contribut. Mineral. Petrol.* **119**, 239–246.
- Widom E. and Shirey S. B. (1996) Os isotope systematics in the Azores: implications for mantle plume sources. *Earth Planet. Sci. Lett.* **142**, 451–465.
- Widom E., Hoernle K. A., Shirey S. B. and Schmincke H.-U. (1999) Os isotope systematics in the Canary Islands and Madeira: lithospheric contamination and mantle plume signatures. *J. Petrol.* **40**, 279–296.
- Woodhead J. D. (1996) Extreme HIMU in an oceanic setting: the geochemistry of Mangaia island (Polynesia), and temporal evolution of the Cook-Austral hotspot. *J. Volcanol. Geotherm. Res.* **72**, 1–19.
- Yaxley G. M. and Green D. H. (1998) Reactions between eclogite and peridotite: mantle refertilization by subducted oceanic crust. *Schweiz. Mineral. Petrogr. Mitt.* **78**, 243–255.
- Zindler A. and Hart S. R. (1986) Chemical geodynamics. *Ann. Rev. Earth Planet. Sci.* **14**, 493–571.
- Zoller W. H., Parrington J. R. and Kotra J. M. P. (1983) Iridium enrichment in airborne particles from Kilauea volcano. *Science* **222**, 1118–1121.

Associate editor: Frederick A. Frey